BrightnESS

Building a Research Infrastructure and Synergies for Highest Scientific Impact on ESS

H2020-INFRADEV-1-2015-1

Grant Agreement Number: 676548

Deliverable Report: D4.14 “Large Area Detector Spectrometry”

1 Project Deliverable Information Sheet

BrightnESS Project	Project Ref. No. 676548	
	Project Title: BrightnESS - Building a Research Infrastructure and Synergies for Highest Scientific Impact on ESS	
	Project Website: https://brightness.esss.se	
	Deliverable No.: 4.14	
	Deliverable Type: Report	
	Dissemination Level:	Contractual Delivery Date: 31.08.2018
		Actual Delivery Date: 24.08.2018
	EC Project Officer: Mina Koleva	

2 Document Control Sheet

Document	Title: BrightnESS_Deliverable_4.14 –Large area detector spectrometry	
	Version: 1.0	
	Available at: https://brightness.esss.se	
	Files: 2	
Authorship	Written by	Anton Khaplanov (ESS, WP4)
	Contributors	Isaak Lopez Higuera, Alessio Laloni, Richard Ammer, Alexander Backis, Anders Lindh Olsson, Emelie Haettner, Pablo Costas Franco, Judith Freita Ramos, Ioannis Apostolidis, Carina Höglund, Linda Robinson, Per-Olof Svensson, Chung-Chuan Lai, Martin Shetty, Morten Jagd Christensen, Vendula Maulerova Richard Hall-Wilton (ESS), Bruno Guerard, Fabien Lafont, Victor Buridon, Jean-Claude Buffet (ILL), Gregoire Fabreges (LLB), Mario Koenen (FZJ), Matthew B Stone, (SNS)
	Reviewed by	Anne Charlotte Joubert, Richard Hall-Wilton
	Approved by	BrightnESS Steering Board

3 List of Abbreviations

ESS	European Spallation Source
ILL	Institut Laue-Langevin
MG	Multi-Grid
CSPEC	Cold Chopper Spectrometer at the ESS
T-REX	Bispectral Chopper Spectrometer at the ESS
CRISP	Neutron reflectometer instrument at ISIS Neutron and Muon Source
SNS	Spallation Neutron Source at Oak Ridge National Laboratory
CNCS	Cold Neutron Chopper Spectrometer at the SNS
MG.CNCS	Multi-Grid at CNCS
TRL	Technology Readiness Level
SEQ,SEQUOIA	Fine-Resolution Fermi Chopper Spectrometer at the SNS
MG.SEQ	Multi-Grid at SEQUOIA
VOR	Versatile Optimal Resolution chopper spectrometer at the ESS
PCB	Printed circuit board
CF	Connection fittings
EWCON	Euro Weld Consulting
CT1	Beam line at the ILL
ToF	Time of Flight
FEM	Finite element method

4 Contents

1 Project Deliverable Information Sheet 2
2 Document Control Sheet 3
3 List of Abbreviations 3
4 Contents 4
5 Executive Summary 5
6 Report on Implementation Process and Status of Deliverable 6
7 Technical Content 6
7.1 Multi-Grid detector development 6
7.2 Operation in Vacuum 6
7.3 MG.SEQ prototype and test 8
7.3.1 MG.SEQ Test of the Vessel design 8
7.3.2 Grid Configuration and Coating Options 11
7.3.3 MG.SEQ Test of Grid configurations 12
7.4 Optimisation for Thermal Instrument 13
7.5 Low-Pressure Operation 13
7.6 Progress on CSPEC detector design 14
7.6.1 Detector interfaces for CSPEC 15
7.6.2 Detector installation in CSPEC 16
7.7 Progress on T-REX detector design 17
7.7.1 Detector installation in T-REX 18
8 Conclusion 18
9 Bibliography 19
10 Appendix 1: 19

5 Executive Summary

The Multi-Grid (MG) detector has been chosen as the baseline detector for the two ESS Direct Geometry spectrometers, CSPEC and T-REX. This decision has been based on the characterization of the MG design that took place during the CRISP project as well as at the beginning of the BrightnESS project [1, 2, 3, 4, 5, 6, 7, 8]. This characterization development stage had been concluded with the test using an MG detector, MG.CNCS at the CNCS instrument at the SNS. This detector is described in the Deliverable 4.5. The results are presented in [1]. The present deliverable focuses on the production and the tests of the key technology demonstrations for the implementation of the MG in the detailed design of the ESS instruments. The conclusion of this deliverable is a detector design successfully brought to Technology Readiness Level (TRL) 8-9.

In order to develop the remaining technological aspects of the implementation of the MG detector, following tasks have been completed. The MG detector MG.SEQ has been designed, built and tested by a collaboration between the ESS and the ILL. Further, a low-pressure gas circulation system has been designed and tested at the ILL. Together, these developments demonstrate the techniques necessary for the implementation of the detector in CSPEC and T-REX, and potentially in VOR at a later stage of the construction of the ESS. The MG.SEQ detector furthermore enables the demonstration of the MG operation at a thermal to epithermal neutron energy range that previously could not be measured due to the challenges of installing the MG at an appropriate instrument.

The specific techniques that have been developed and understood during the MG.SEQ work include: the design of a gas vessel for the detector that is compatible with both vacuum and overpressure; the welding techniques needed to successfully construct such a vessel; construction of grids using hydrogen-free materials only; design of the feedthrough from the external atmosphere to the detector placed in vacuum; grid coating options and grid size options. Furthermore, the design incorporates an electronics enclosure that can easily be customised for more than one type of the front-end readout electronics.

The development of the low-pressure gas circulation system enables the operation of the MG detector in a vacuum chamber with a low pressure in the detector interior while enabling continuous flushing of the detector gas. This development makes it possible to significantly reduce the mechanical requirements on the detector vessel, which in turn allows to reduce the thickness of the detector window and the dead areas between detectors, thereby increasing the detector efficiency and the signal-to-noise ratio as well as increasing the detector coverage.

The design of CSPEC and T-REX is currently proceeding and taking advantage of the experience in developing the technologies described above. Particular impact can be seen in the design of the detector vessels and feedthroughs of both instruments. The results of the upcoming test at the SEQUOIA instrument at the SNS will finalise the characterization work by demonstrating the detector performance at short neutron wavelengths as well as give a comparison of the influence of the coating strategy on the signal-to-noise ratio.

The overall result of this deliverable, and more generally of task 4.3 of BrightnESS, is a mature detector technology, which is ready for construction and implementation for the chopper spectrometers at ESS. Additionally, this novel detector technology, as a performant He-3 replacement technology, is attracting interest for applications outside of ESS.

6 Report on Implementation Process and Status of Deliverable

The work completed within the current deliverable builds on the results of the previous deliverables D4.5 and D4.10 [12, 13], which were focused on simulations and the detector development. The current work brings the Multi-Grid detector development to a conclusion where the techniques and the methods of the detector production for the ESS instruments become clear. The MG.SEQ prototype has been designed and built. The lessons learned from this process are now being implemented in the design of CSPEC and T-REX detectors.

The first step for the design of the MG detectors for CSPEC and T-REX has been the integration design. The detectors need to be installed in a vacuum tank in each instrument. They must then be connected to the services and the data acquisition systems outside of the tank. There must also be a method of handling the detectors, whose weight is on the order of half a ton or more, safely and positioning them with a high-degree of accuracy. This required to define a concept of the detector designs and the tank designs and to proceed to the detailed design of the interfaces. It is then necessary to lock the outer space envelopes of the detectors and their positions within the tank, however within these envelopes, the design can remain at a conceptual state.

The reason to proceed quickly to the detailed integration design is that the tank is an especially long-production item and will have to be tendered relatively early in the instrument construction process. The interfaces to the detector need to be clearly defined at the beginning of the tender process.

Over the course of the completion of this deliverable, the production of the prototype MG.SEQ detector has been completed in parallel with the integration design. MG.SEQ is designed for an imminent test on the SEQUOIA at the SNS. While being constrained by the space available for a test in this instrument, the detector is built with several features of CSPEC and T-REX and has significantly contributed to the design of the final ESS detectors. The work is continuing on the detailed designs of the CSPEC and T-REX detectors based on this progress. Further work is currently being performed on testing MG.SEQ at the SEQUOIA instrument at the SNS.

7 Technical Content

7.1 The Multi-Grid detector development

During the BrightnESS project final stage, The Multi-Grid prototype MG.SEQ has been designed and constructed. This detector is the final development prototype that represents the step in development before the construction of detectors for CSPEC andT-REX. The outstanding points that had to be demonstrated were the design of a suitable vacuum vessel, the comparison of the options for the construction of the grids, the optimisations for a thermal instrument and the possibility of a low-pressure operation. The following sections describe in detail how these points have been achieved.

7.2 The Operation in Vacuum

The MG detector must be placed in a large vacuum tank in both CSPEC and T-REX due to the requirements of the low neutron scattering as well as the cryogenic sample environments.

This presents a challenge for the mechanical design, since the MG detector must house the grid modules with large dimensions inside a gas volume. In the first approach, this requires a rectangular gas chamber, which has 1 atmosphere of $ArCO_2$ inside and vacuum outside. In other words it must support 1 bar of overpressure.

The minimum dimensions of the detector vessel needed are 30cm*30cm*3.5m (W*D*H) for the case of the CSPEC detector. While the height is the largest dimension, it is mainly the two smaller dimensions that present the challenge. The detector vessel can essentially be seen as a long pipe with a near-rectangular cross section. For heights greater than 1m, the deformations are constant along the entire height. Considering a pressure difference of 1 bar, the force on the walls of the vessel is approximately 3 tons per 1 meter of height. The vessel must be able to withstand this pressure. Deformations are acceptable, but must be such that the adjacent detectors do not clash and the vessels do not clash with the grids inside. Furthermore, it must be built using aluminium in order to ensure the optimal neutron transparency.

This challenge has been solved by combining a rigid back-plate with a 4-mm thick sheet that is bent and forms the sides and the front window (the detector vessel cross section and the bent sheet can be in detail seen in the sec. 7.6 on the fig. 9) . The rounded bend ensures that the front corners of the vessels are much more free of stress than they would be in the case if the window and the sides had been welded together from separate sheets at the right angle. It also minimises the need for long welds. The two above parts form a tube of the necessary height. The tube is then terminated with a welded flange on either end. The flanges of different sizes are used at each end, one with the outer dimension equal to the cross section of the tube and one with the inner dimension equal to the cross section of the tube. The larger flange is used to assemble the detector, since the grid dimension is such that the grids cannot pass through the smaller flange. The smaller flange is nevertheless needed in order to make connections to the end of the grid modules as well as for the maintenance of the module.

Finally, an electronics enclosure is connected to the main detector volume. The two volumes must be separate since the detector volume is filled with $ArCO_2$ gas mixture, which must remain at a constant temperature in order to ensure stable neutron detection conditions. The electronics enclosure can be filled with any gas, most conveniently air, which will be heated by the power output of the electronics. An important note is that while the two volumes must be separated and must have their individual gas supplies and flows, the separation is free of a pressure difference and is not sensitive to small leaks. It can therefore be made in a cheap and simple way. This is important, as a very large number of the electronics feedthroughs must pass this separation – those carrying the signals from each individual grid and each individual wire (1000-2000 in total). Ensuring a vacuum-grade feedthrough for this number of connections would require a large number of very expensive feedthroughs. Our solution makes sure that both the cost and space are conserved by using the cheap high-density connectors. The separation itself is provided by a PCB mounted between the two volumes.

The electronics enclosure is then connected to the exterior of the vacuum tank using a wide bellows, such as a CF, or ISO-K 100, 63 bellows (the MG.SEQ electronics enclosure tested at SEQUOIA is described in the sec. 7.3.1 fig. 3, for the planned design for CSPEC enclosure, see sec. 7.6.1, fig. 11). This provides sufficient amount of space through which all the detector services can pass, including:

- High voltage
- Low voltage
- Signals

- Gas flow lines
- Coolant lines
- Monitoring lines

Note that none of the above connections require vacuum feedthroughs. They are housed in the atmosphere until they reach the detector volume.

With this strategy, the detector envelope as a whole – the detector volume, the electronics enclosure and the bellows – is vacuum-tight, however, internally, no vacuum-grade components are needed. This also makes the detector robust to material choices, since the gas circulation ensures gas purity even if outgassing is present.

Another important aspect of the detector construction is the support and the possibility for the alignment of the detector upon installation in an instrument. The thick back-plate used in the construction of the detector vessel takes the load due to the weight of the grid modules and other components of the vessel. The detector can be either suspended from a mount on the back of the detector (the CSPEC solution, see sec. 7.6.2) or it can be stood on a supporting table (the T-REX solution, see sec. 7.7.1). Either solution allows decoupling the detector from the deformations of the vacuum tank due to the vacuum pumping, since the detector is partially free and cannot be deformed or displaced by the flexing of the tank.

7.3 The MG.SEQ prototype and test

A prototype detector called MG.SEQ is a set of the 3 detectors that have been built for a test at the SEQUOIA at the SNS. This detector prototypes a number of key design features for CSPEC and T-REX. It is currently being installed at SEQUOIA and will test the performance of the MG at a thermal neutron spectrum. It will be the first MG detector to operate in vacuum.

Figure 2. An MG.SEQ placement for the test at SEQUOIA. The MG.SEQ is the triple detector in the lower-right corner of the array. On right, photograph of the SEQUOIA He3 detector array.

7.3.1 The MG.SEQ Test of the Vessel design

The MG.SEQ has implemented these aspects, demonstrating their feasibility and the techniques needed to achieve them. The vessel cross section is very similar to that of the CSPEC vessel and uses the same idea of a thick back-plate combined with a bent front sheet.

The installation location in the SEQUOIA instrument is shown in figure 2. The available height is limited to just over 1m. Therefore the MG.SEQ was designed with the electronics enclosure at the rear of the detector. The space behind the detector is not limited and this way the available height can be fully used for the detection. In CSPEC, the detector will be mounted adjacent to the wall of the vacuum tank; therefore the electronics enclosure will be placed below the detector. Both options for the electronics enclosure placement are still open in the case of T-REX. Nevertheless, the method of both connecting the electronics enclosure to the detector and to the exterior of the tank will be very similar and will benefit from the experience from the MG.SEQ. The design of the MG.SEQ is shown in figure 3.

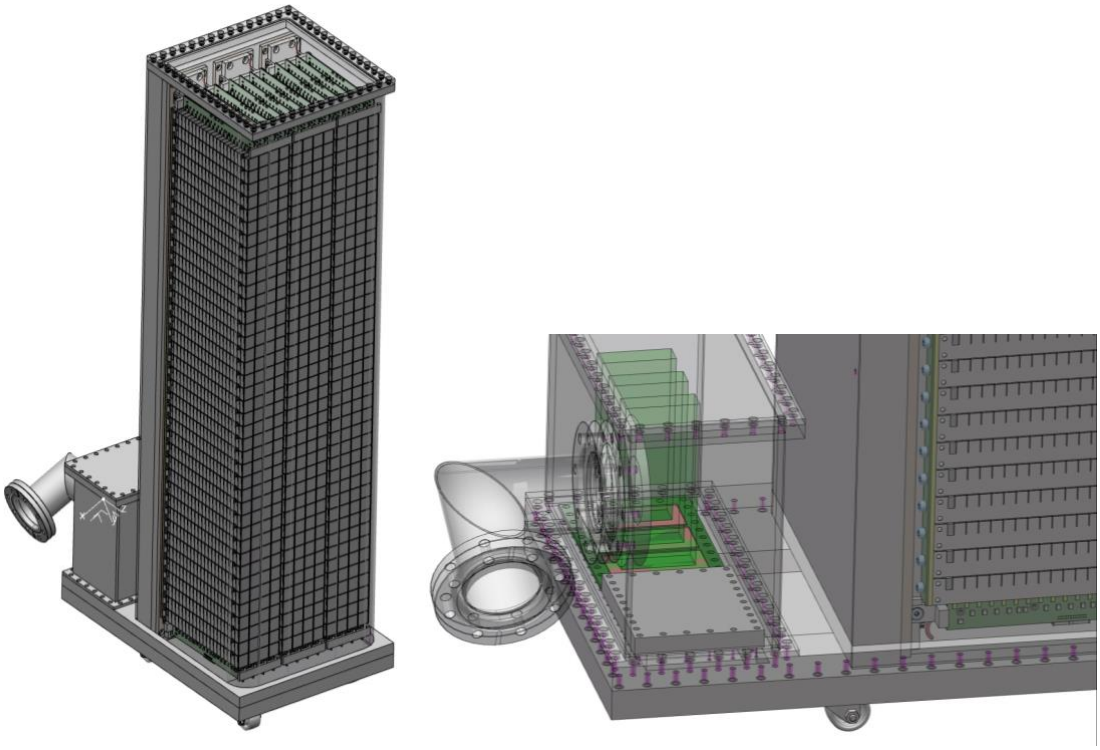

Figure 3. Design of 1 of the MG.SEQ detectors. On the right, the close-up of the electronics enclosure and the beginning of the bellows connecting the detector to the tank exterior.

The manufacturing of the MG.SEQ vessel has provided a range of valuable information for the design of the larger CSPEC and T-REX vessels. The points that need particular attention in the design are the long welds connecting the back- and front-sections of the vessel as well as the corners of the vessels.

Finite element method, FEM, simulations have been performed on the designs of the MG.SEQ, CSPEC and T-REX vessels. These show the stresses and deformations of the vessels due to the overpressure forces. Observations of the MG.SEQ vessel at overpressure has confirmed these simulations. It has further confirmed that the stresses do not exceed the yield point of the aluminium alloy used.

The tests on the MG.SEQ have been performed so far by vacuum pumping the detector to the pressure of 1e-4 mBar and by over-pressuring it to 1.2 Bar. The latter has been repeated at least 10 times for each of the 3 detectors. In each case, the pressure loss has been measured over time in order to estimate the leak rate. The resulting leak rate is expected to allow operation at 1e-5mBar in the SEQUOIA tank, considering the installed pumping system. This pressure is somewhat below the target for the current T-REX requirements and

compatible with the CSPEC requirements. There are several improvements foreseen in order to decrease the leak rate significantly. This will be achieved primarily by replacing gaskets with o-rings and by milling the seal surfaces after the welding of the vessels, rather than prior.

A new feature that was introduced in the MG.SEQ and will be used in CSPEC and T-REX are rails used to support and install the grid modules. These make it easy to install and access the grids modules as needed, while providing the accurate repeatable placement of the modules.

The 3 units of the MG.SEQ have been assembled and tested in the ESS Utgård facility in Lund, figures 4 and 5. Most of the vacuum and leak tightness tests were performed in collaboration with EWCON, who also performed all of the welding of the vessels. A first neutron beam test of the MG.SEQ was done at the CT1 beam line at the ILL, see figure 6.

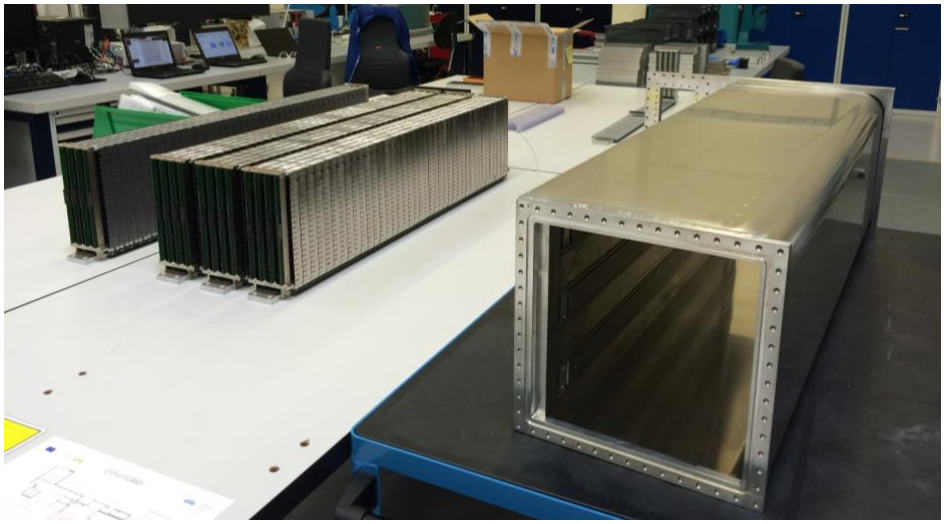

Figure 4. MG.SEQ Grid modules and a detector vessel.

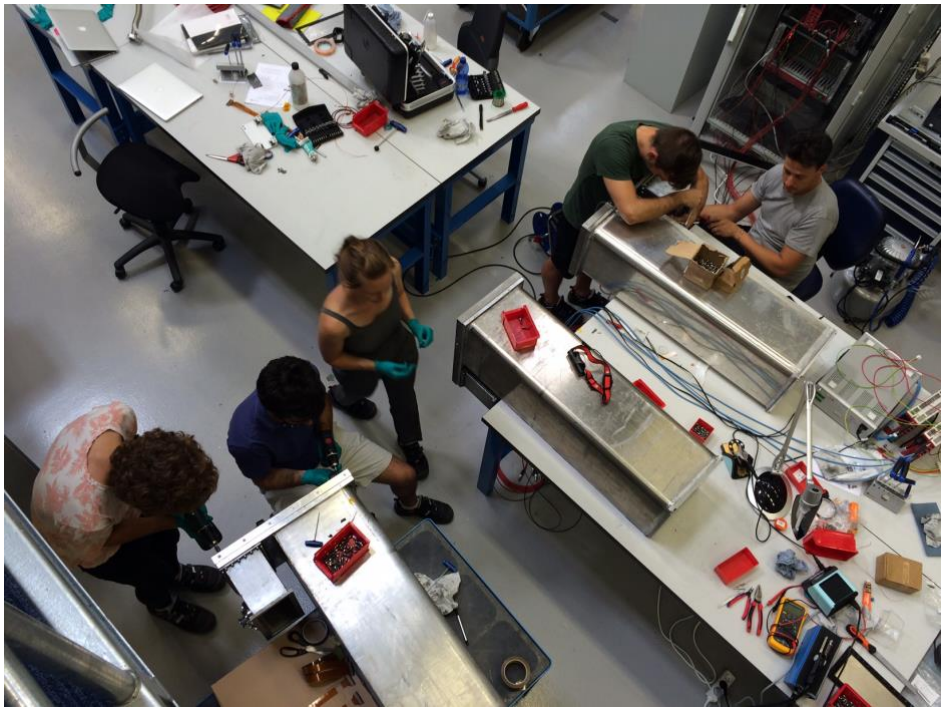

Figure 5. Construction of MG.SEQ detectors in ESS Utgård facility

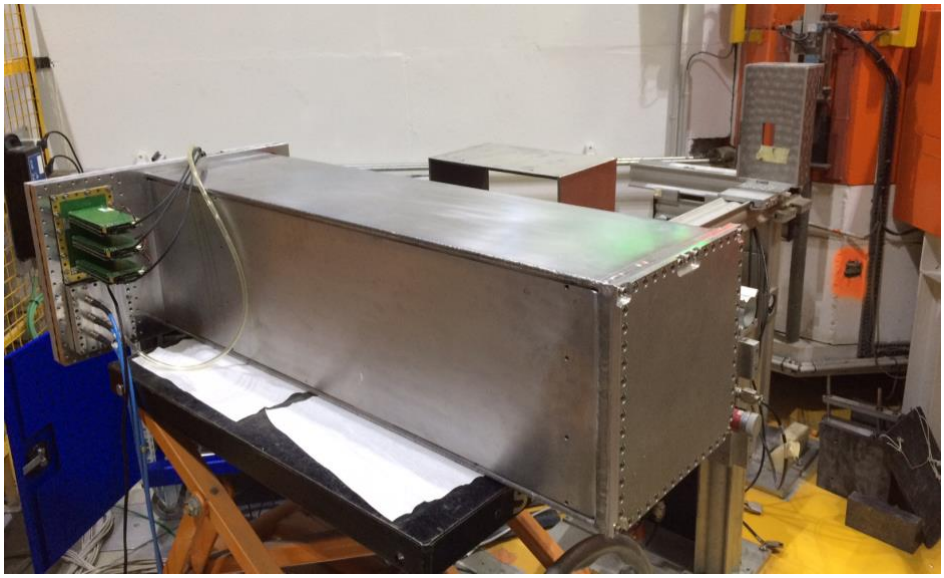

Figure 6. The MG.SEQ during a beam test at ILL

7.3.2 The Grid Configuration and the Coating Options

Several grid sizes have been used over the course of the development of the MG detector. For CSPEC and T-REX we will use a blade dimensions of 150mm * 24mm. This offers a good balance between several parameters:

- Number of blades that can be coated per run in the ESS coating workshop
- Complexity and robustness of the grid construction
- Desirable active area coverage

In the MG.SEQ, 2 grid sizes have been implemented: one with a 90mm-long blade, and one with a 270mm-long blade, see figure 7. The smaller grids have been built in the ESS and the larger in the ILL. The smaller grids have less dead material and allow the additional shielding to be placed between the grids, while the larger grids require a rigid outer frame, however, have 3 times fewer inter-grid gaps, and therefore better coverage overall. We will shortly experimentally verify the performance differences of the two approaches during the SEQUOIA beam time.

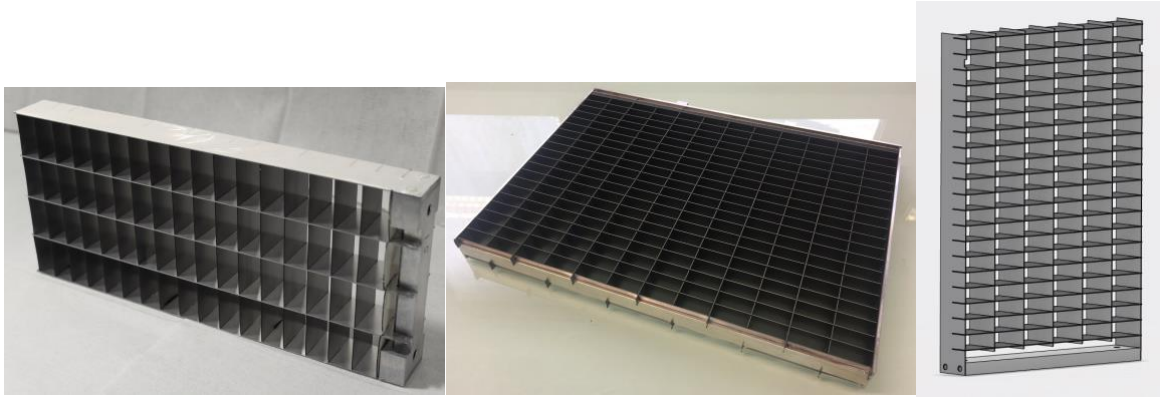

Figure 7. Grids – from left to right: 4-cell wide grid (MG.SEQ, CRISP prototype), wide 12-cell grid (ILL version of MG.SEQ), 6 cell grid design (CSPEC, T-REX).

A further option for the grid design is the presence of the B_4C coating on the radial (parallel to the incoming neutrons) blades of the grids. The normal blades are always coated, and contribute with the bulk to the detector efficiency. The radial blades only contribute to additional efficiency at angles matching their positions. However, they further contribute to the internal shielding of the detector from scattered neutrons by both absorbing and detecting neutrons that have scattered in the detector inactive materials. The benefit of this effect is not readily understood analytically, it is therefore essential to gauge it in a measurement. The SEQUOIA setup suits this perfectly, since the ToF measurement is perfect for analysing the scattering contributions and the wide range of neutron energies that can be used will give a good understanding of the effect on the efficiency and the background.

7.3.3 The MG.SEQ Test of Grid configurations

The MG.SEQ was designed to cover approximately a $1m^2$ area. This is achieved using 3 individual detector vessels with 3 grid modules in each. We have used this redundancy to test several grid configurations. The 3 detectors are assembled using following grids:

- Detector 1 – grids with only normal blades coated
- Detector 2 – grids with both normal and radial blades coated
- Detector 3 – grids with both normal and radial blades coated, large grids

Large grids are the grids manufactured at the ILL. These are 3 times wider than the grids of detectors 1 and 2. They occupy the same space and have the same total number of pixels as the 3 grid modules in detectors 1 and 2. Note that each detector has the same number of normal boron layers – 40 layers as per thermal optimisation. The difference is in the presence of the coating on the radial blades and the distribution of the dead spaces.

These configurations allow us to compare experimentally the benefit of coating the radial blades. Theoretically, this coating should both contribute with an additional efficiency for neutrons, which travel close to a cell boundary. It should further limit the effect of the scattering, as neutrons scattered in the aluminium substrates will have a higher chance to be stopped by boron layers closer to the scattering point.

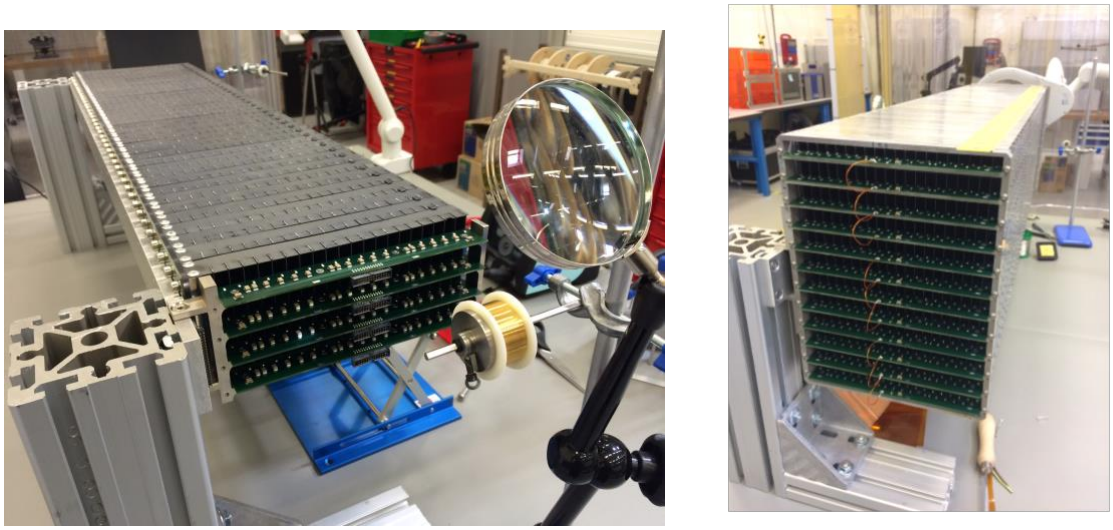

Figure 8. On the left, a module of regular grids in the wiring setup. On the right, the module of large grids.

The use of the large grid has the advantage that the dead area of the detector is reduced, as is the number of the grid readout channels. The drawback is that a grid with a larger area can more easily be saturated by a large neutron flux. Additionally, it has a thicker front element that will attenuate the neutron flux. The MG.SEQ test will allow to evaluate these aspects experimentally.

All the blades were coated in the ESS workshop in Linköping, which is dedicated to Boron-10 Carbide coating on the aluminium and other substrates [9, 10, 11].

7.4 The Optimisation for Thermal Instrument

The earlier MG test at the CNCS [1] was performed using cold neutrons available at the CNCS, primarily with energies up to 15 meV (and only one low-statistics point at 80 meV). SEQUOIA offers much higher energy of the incoming neutrons, up to 1500 meV, well into the epithermal range. The test will take advantage of this to extend the MG characterization to this energy. The detector has been designed with the same optimisation of the boron layer thicknesses as that foreseen for T-REX, using 1Å as the centre of the region of interest. This results in the following blade arrangement.

- 4 blades of 1.0 µm B_4C coating
- 10 blades of 1.25 µm B_4C coating
- 6 blades of 2.0 µm B_4C coating

In this way, the detector is set for the best possible performance in SEQUOIA, and will verify the predicted efficiency for T-REX.

7.5 The Low-Pressure Operation

A further line of research for the implementation of the MG has been concluded at the ILL. It has been shown that the MG detector can successfully operate at an internal pressure as low as 50 mbar. In order to achieve this, a dedicated gas flow and a regulation system is needed. This too has been designed. The details of the design and operation of this system are presented in an appendix to this report.

For a 1-atmosphere detector, it is sufficient to supply a constant flow at the inlet and have the outlet open to the atmosphere. By contrast, in order to operate the MG at a low gas pressure, it is necessary to regulate and monitor both inlet and outlet pressures. The system therefore includes connections to vacuum, to the pressurised gas, to the detector and to the detector ambient environment. Computer-controlled flow regulators maintain the desired detector pressure at the detector outlet and provide a slight overpressure at the inlet. The system has been made fully automated.

This development makes it possible to operate an MG detector at a pressure that is significantly closer to vacuum than to the atmosphere, and thereby reduce necessary thickness of the detector vessel. The advantages include:

- Lower scattering of neutrons in the detector window and side walls

- Lower weight of the detector
- Lower requirements on the welds

The low pressure option is not currently implemented in the design of CSPEC and T-REX, due to the regulatory requirements for the vacuum vessel safety qualification for operation. However, with a more unified approach to the vacuum tank and the detector design, the necessary qualification can become more realistic. In view of the potential performance and technical advantages, consideration of its implementation will be given at a later stage and at other facilities.

7.6 The Progress on CSPEC detector design

The advances made on the MG detector technology are now being implemented into the design of the MG detector for CSPEC. The configuration of the CSPEC detector is similar to that of the MG.SEQ. The detector vessel will have an almost identical cross section, with a rigid back-plate and a bent sheet forming the front window and side walls, se figure 9. The vessel interior will be occupied by two grid modules, which are 6 cells wide, resulting in the same total width and the same pixel density as in the MG.SEQ. The differences are the height of the detector, which in case of CSPEC will be 3.5 meters, and the position of the electronics enclosure, which will be below the detector volume, rather than behind as in the MG.SEQ.

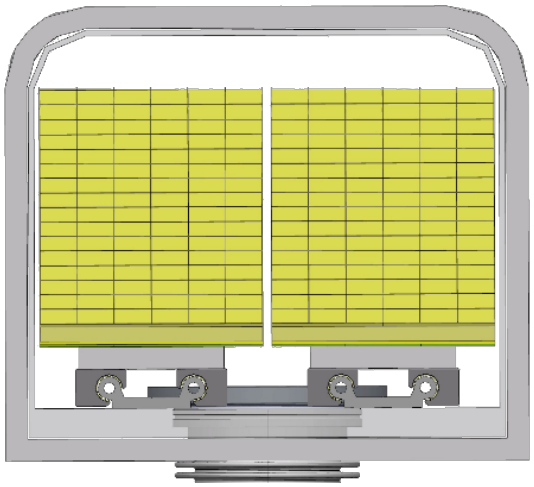

Figure 9. A horizontal cross section of the CSPEC detector vessel, showing placement of the 2 grid modules. Here, neutrons arrive from the top of the figure.

A configuration where 140 grids make up the height of the detector array and 54 grid modules tile its width has been chosen. The grids have 6 cells in width. The detector array is shown in figure 10. The cell dimensions are 25x25x10 mm^3 (defined as a center-to-center pitch). Two detector modules will share a single detector vessel, resulting in a total of 27 detectors needed to complete the instrument. Each detector will be angled to face the sample, however the two modules within each detector will be parallel. This is possible, since with only two modules all cells will have a full line of sight to the sample.

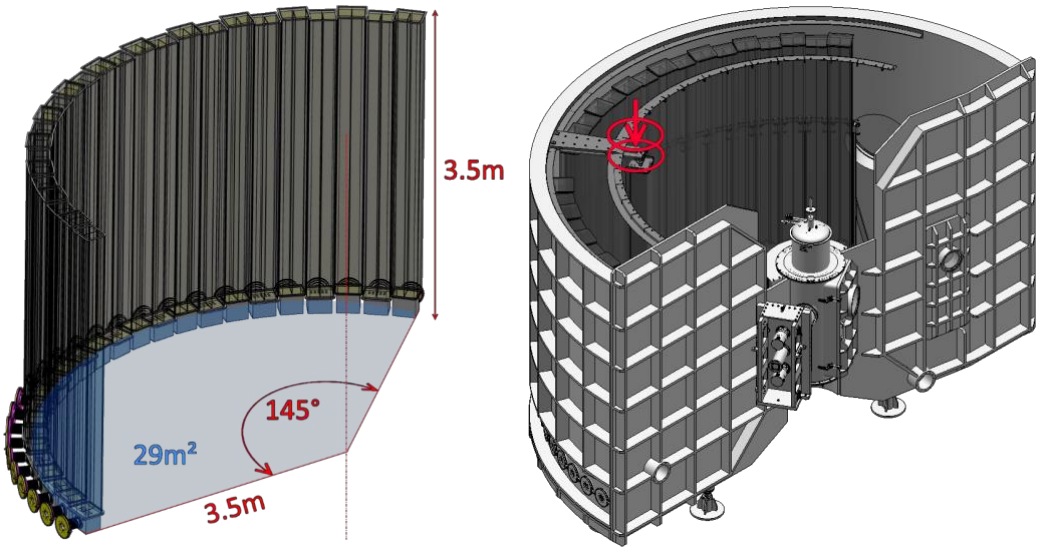

Figure 10.The detector array design for CSPEC. On the right, the design including the vacuum tank and the installation system.

7.6.1 Detector interfaces for CSPEC

Since the CSPEC detector tank is being designed specifically for the MG detector, it has been possible to design the link between the detector and the tank exterior in such a way that the connections are very short and with a large port between the electronics enclosure and the exterior. As shown in figure 11, the detector has 100-mm bellow preinstalled. This bellow links to a dedicated flange on the detector tank rear wall. The interior of the electronics enclosure thus forms a pocket of the atmosphere within the tank. The proximity to the exterior allows several cooling options that do not require any cooling lines inside the vacuum. Indeed, all connections to the detector can be made via this air pocket, including:

- Detector gas supply and exhaust
- Detector high voltage
- Electronics low voltage
- Digital signals out
- Electronics cooling

Since none of the above connections enter the high vacuum of the tank, they do not require vacuum grade feedthroughs. The connections that enter the detector volume from the electronics enclosure are:

- Detector gas supply and exhaust
- Detector high voltage
- Analogue signals out

These connections require feedthroughs, however, the only requirement for these feedthroughs is that they separate the gas of the detector volume and the air at zero pressure difference. These can therefore be executed cheaply.

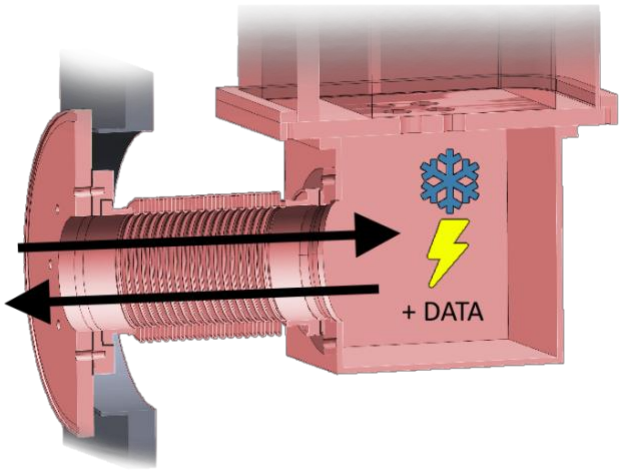

Figure 11. The link between the exterior of the vacuum tank and the detector electronics enclosure.

7.6.2 Detector installation in CSPEC

The CSPEC detector is installed using a rail system as shown in figure 13. The detector is lowered into the tank using a large flange on the top surface of the tank. It is then connected to the rail and can be translated into any final position without interfering with other detectors.

When brought to the final position, the detector is suspended on a support using a ball joint. The support provides several positioning points, which allows the detector to be aligned. The supports rest on the interior of the detector tank bottom surface. FEM simulations show that the bottom surface deforms less than the side walls of the tank. However, some deformation does exist. Therefore the detector position will be carefully adjusted, so that it is aligned correctly once under vacuum.

Maintenance of the detector will in most cases involve the removal of the detector from the vacuum tank. A possibility for a minor maintenance of the electronics and the connections is additionally possible by using an access flange on the front of the electronics enclosure (not in the current drawing yet).

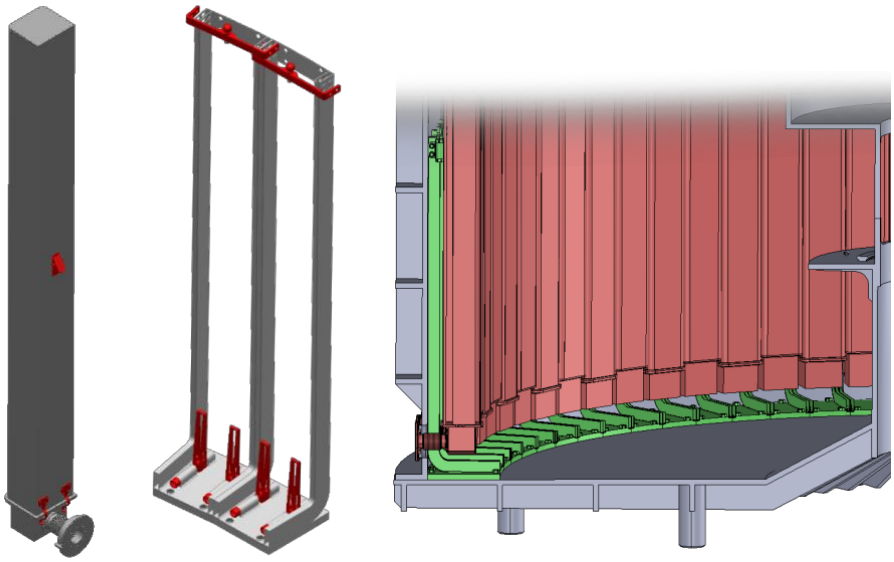

Figure 12. Support mechanics of the CSPEC detectors.

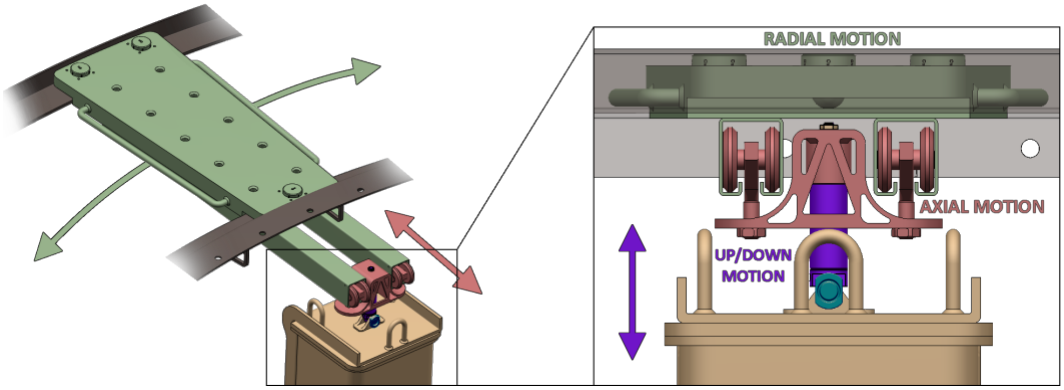

Figure 13. The rail system that moves detectors within the CSPEC vacuum tank.

7.7 The Progress on T-REX detector design

The T-REX detector array will be at 3 meters from the sample and will have a 2.2m height and a 180-degree total coverage. This will be instrumented with a total 60 grid modules of 88 grids each. The cell dimensions, 25x25x10 mm3 will be used as in CSPEC, however, the grid depth will be increased to 20 cells due to the higher-energy spectrum.

The T-REX team has chosen a different approach to the vessel of their Multi-Grid detector. Ten wider vessels will be built, housing 6 modules each. The reduced total number of detectors results in an increased complexity of each vessel. The grid modules will have to be angled individually within the vessel to face the sample. Reinforcement webbing will have to be used between the grid modules in order to support the thin entrance window. The advantage is in a much smaller number of interfaces needed to the outside of the vacuum tank. Another reason this arrangement is feasible in T-REX, is due to the extra space behind the detectors available in the T-REX design, which will enable access to the detectors both from the front as well as from the rear.

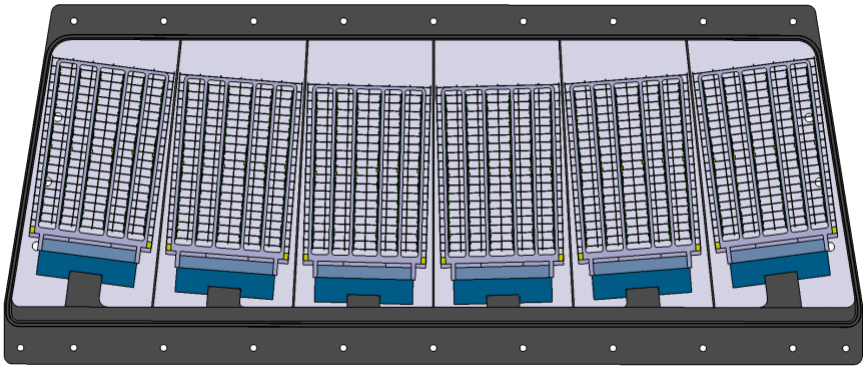

Figure 14. Horizontal cross section of the T-REX detector vessel showing grid module arrangement. Neutrons arrive from the top in this figure.

7.7.1 The Detector installation in T-REX

The T-REX detectors will stand on a support coupled directly to the experimental hall floor, ensuring that the installation alignment is preserved under vacuum. The vacuum tank will be decoupled from these supports using bellows-enclosed feedthroughs. The supports will provide all the flexibility to adjust the detector position. Bellows will also be used at the top of the tank to link the detector to the exterior. The tank will be equipped with a rail system, which will carry the detectors in or out of the tank as necessary, similarly to CSPEC. The detectors will enter the tank via a side door. Further details are currently being developed as the design of the detector tank is being finalised.

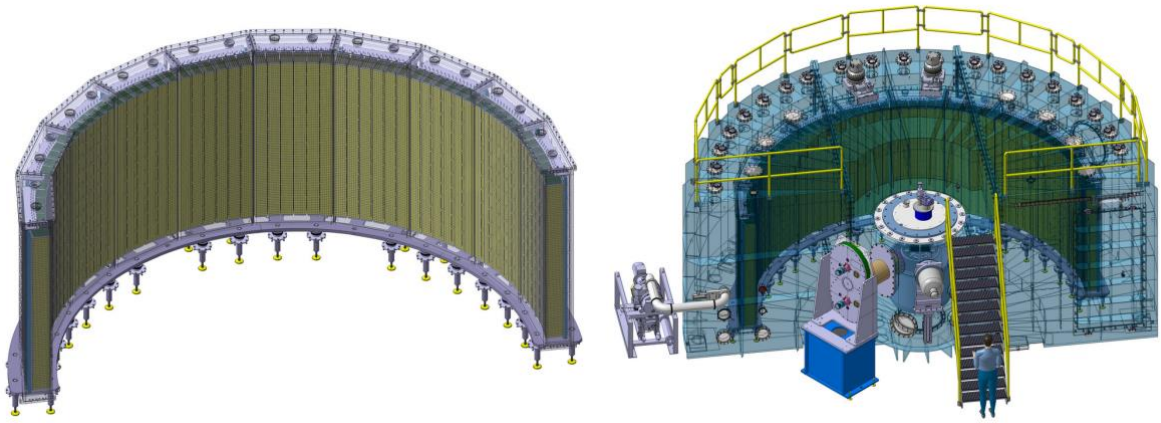

Figure 15. The detector array of T-REX including the floor-coupled support. On the right, detectors installed in the vacuum tank.

8 Conclusion

The results of the work on the Multi-Grid detector for large-area detectors of the ESS spectrometers, CSPEC and T-REX, have been presented in this deliverable report. The development has been performed via the MG.SEQ project. This has helped to prototype the

key design features of the final detectors. The MG.SEQ detector has been constructed and has undergone mechanical and basic detection testing. It is currently being installed for an in-beam test. Additionally, a gas circulation system has been designed. It allows to operate Multi-Grid detector at pressure below atmospheric, thereby simplifying the mechanical requirements in future detectors of this kind. The continuing work now focuses on a detailed design for the detectors of the ESS instrument.

9 Bibliography

[1] A. Khaplanov et al. "Multi-Grid Detector for Neutron Spectroscopy: Results Obtained on Time-of-Flight Spectrometer CNCS", 2017 JINST 12 P04030, doi:10.1088/1748-0221/12/04/P04030, https://arxiv.org/abs/1703.03626
[2] A. Khaplanov et al., Multi-Grid Boron-10 detector for large area applications in neutron scattering science, arXiv:1209.0566 (2012)
[3] J. Correa et al., 10B4C Multi-Grid as an Alternative to 3He for Large Area Neutron Detectors, Trans. Nucl. Sc. (2013) DOI: 10.1109/TNS.2012.2227798
[4] J. Correa 10B4C Multi-Grid as an Alternative to 3He for Large Area Neutron Detectors PhD thesis, ILL and Uni Zaragoza (2012)
[5] B. Guerard et al., 10B multi-grid proportional gas counters for large area thermal neutron detectors, Nucl. Instr. Meth. A (2012) http://dx.doi.org/10.1016/j.nima.2012.12.021
[6] J Birch et al., In-beam test of the Boron-10 Multi-Grid neutron detector at the IN6 time-offlight spectrometer at the ILL J. Phys.: Conf. Ser. (2014) 528 012040 doi:10.1088/1742-6596/528/1/012040
[7] A. Khaplanov et al., Investigation of gamma-ray sensitivity of neutron detectors based on thin converter films J. Inst. (2013) 1748-0221 8 P10025 doi:10.1088/1748-0221/8/10/P10025
[8] A. Khaplanov et al., Investigation of background in large-area neutron detectors due to alpha emission from impurities in aluminium J. Inst. (2015) 10 P10019 doi:10.1088/1748-0221/10/10/P10019
[9] C. Höglund, et al., B4C thin films for neutron detection, J. Appl. Phys. 111(104908) (2012)
[10] C. Höglund et al., 2015 Stability of 10B4C thin films under neutron radiation Radiat. Phys. Chem. 113 14–19
[11] S. Schmidt, et al. "Low-temperature growth of boron carbide coatings by direct current magnetron sputtering and high-power impulse magnetron sputtering", Journal of Materials Science 51, Issue 23 (2016); doi:10.1007/s10853-016-0262-4.
[12] BrightnESS Deliverable D4.5
https://brightness.esss.se/about/deliverables/45-simulation-and-generic-multi-grid-design
DOI: https://doi.org/10.17199/BRIGHTNESS.D4.5
[13] BrightnESS Deliverable D4.10
https://brightness.esss.se/about/deliverables/410-test-technology-demonstrator
DOI: https://doi.org/10.17199/BRIGHTNESS.D4.10

10 Appendix 1:

An automated gas control system to operate safely Multi-Grid detectors at low pressures in vacuum chambers,
F. Lafont

An automated gas control system to operate safely Multi-Grid detectors at low pressures in vacuum chambers

F. Lafont

Introduction

Multi-Grid technology as neutron detectors has already been validated so that two ESS instruments (CSPEC and T-REX) will be equipped with this kind of detectors. One of the big challenge of this technology regards the vessels of the detection volumes. Indeed, being composed of many ^{10}B-based layers, the vessel and volume of a Multi-Grid detector containing the gas is quite large compared to standard ^{3}He tubes. Consequently, the global weight of the system can be high and the reinforcement structures to withstand the differential pressure between the detection volume and the external environment – usually the TOF chamber of the instrument – can become a big issue in terms of dead spaces, weight and design.

One of the advantage of Multi-Grid detectors is their capability to be operated at rather low pressures, typically 1 bar absolute of Ar-CO_2 mix. During the several development phases, particularly at ILL, it has been demonstrated that there were further advantages in terms of counting rate and gamma rays sensitivity to operate the Multi-Grid detector at even lower pressures, typically around 100 mbar. But the main interest in reducing the pressure comes from the possibility to lower the weight and the complexity of the vessel assembly and in the meantime, enlarge the grids of the detector to reduce detection dead gaps.

Building vessels withstanding only overpressure around the sensing gas absolute pressure makes sense but requires an adequate gas control system to guarantee the safety of operation inside the TOF chamber of the instrument. Indeed, if the vacuum of the TOF chamber is broken, the pressure of the detector needs to be quickly adjusted not to be destroyed by a too high overpressure. For the two next instruments at ESS using Multi-Grid, decision has been made to have vessels that withstand 1 bar overpressure to guarantee safety in any case. Nevertheless, there is at this moment no fixed ideas regarding the third one (VOR) that could use also Multi-Grid technology, so the option of lighter vessels can still be discussed which implies that a study about an automated gas control system needs to be made.

This document intends to present the development of an automated gas control system made at ILL. After having given a description of the system, one will focus on the risks analysis regarding the operation of a detector withstanding only 100 mbar overpressure in a vaccum or atmospheric pressure environment.

Then, the programmable logic controller will be detailed as well as the program and the Human-to-Machine Interface I developed to control the different components of the system.

Description of the system

A first scheme of the gas delivery system is given in Figure 1 and all the components are listed below:

List of components:

- TOF Chamber
- Detector: Leakage rate (Virtual valve **Leak**), Manual inlet and outlet valves V_{d_in} and V_{d_out}, WIKA Pressure gauge (0-1 bar abs – 0.1 % FS acc.) PG_{d1}
- Manual vacuum valve V_c
- Root pumps **RP** + N.C. electro-valve $EV_{RP.}$
- Chamber pump P_m + N.C. electro-valve EV_{pm}
- Detector pump P_s + N.C. electro-valve EV_{ps}
- Dry Air bottle + manual pressure regulator + N.C. electro-valve EV_a.
- Gas mix bottle + manual pressure regulator + N.C. electro-valve EV_g.
- Differential Pressure Gauge **DPG**
- High flowrate Safety electro-valve N.O. EV_s
- Dual Valve Pressure Controller for the TOF chamber $DVPC_c$ with an internal pressure gauge.
- Single Valve Pressure Controller for the detector $SVPC_d$, coupled to an external pressure gauge PG_{d1}.
- High flowrate bypass electro-valve N.C. EV_d
- Low (~100 mL/min) and High (~50L/min) volumetric flow rate Flowmeter for gas injection F_{i_LF} and F_{i_HF}
- Low flow (~100 mL/min) Mass Flow controller for detector outlet FC_{o_LF}
- High flow bypass electro-valve for detector outlet EV_{o_HF}
- Humidity sensor **H**
- Temperature Sensor **T°**
- Switches on/off for Low and High Voltage supplies **LV** and **HV**

**Any reference to an electro-valve corresponds here to a pneumatic-valve coupled with an electro-valve in order to have end-switches to know the status of the valve.*

The detector is placed in the TOF chamber. At any time, the extreme limit of differential pressure between the two volume is fixed at 100 mbar (positive or negative). These values should be adjusted regarding the design chosen for the vessels. If for any reason, the value exceeds the limit, the safety electro-valve EV_s is automatically opened. In case of electrical failure, this valve is Normally Open (N.O.).

To regulate the pressure inside the TOF chamber that constitutes a closed volume, the system is provided with a dual valve pressure controller $DVPC_c$. The pressure is measured by the internal sensor, at the outlet of the controller. Thus, the piping to the chamber should be done carefully, minimizing the pressure losses along the line to get a correct pressure information. The supply is connected to fresh air and the exhaust to the regulation pumping station P_m.

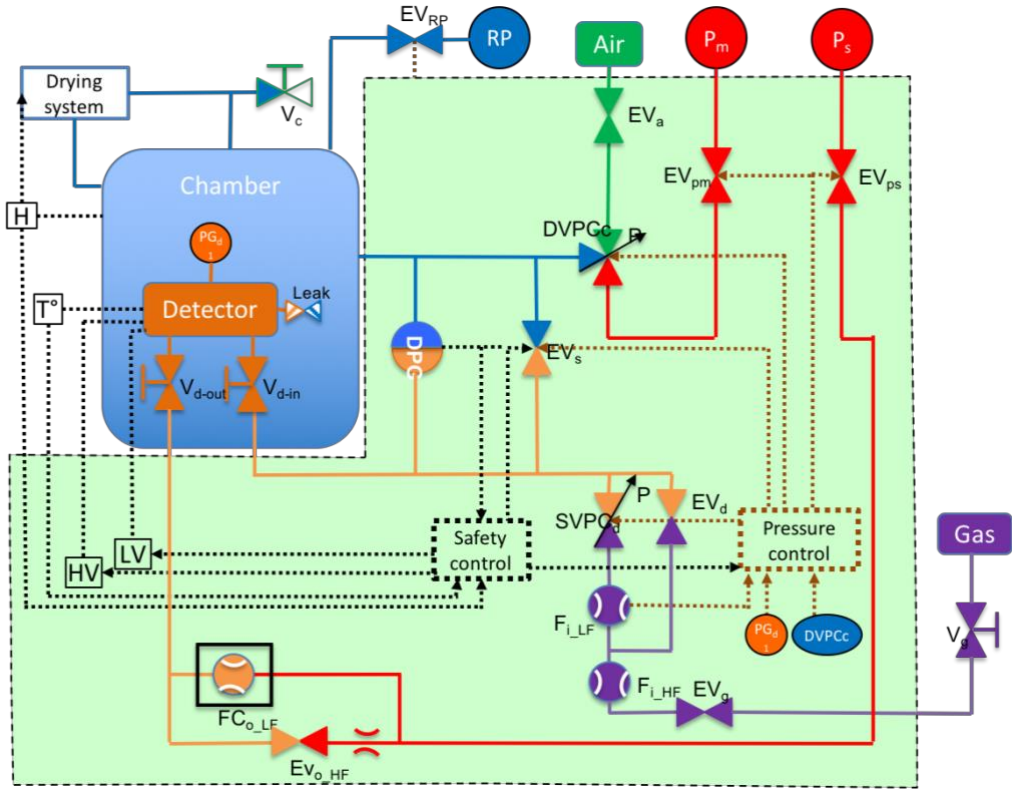

Figure 1: Scheme of the gas delivery system

To regulate the pressure inside the detector, the system is equipped with a single valve pressure controller **$SVPC_d$** connected to the gas mix supply. The pressure information is returned by **PG_{d1}** to the controller. The flow of gas is monitored thanks to two flowmeters **F_{i_LF}** and **F_{i_HF}**, each of them being dedicated for different ranges of flowrate – respectively 100 mL/min and 50 L/min (at Standard Temperature and Pressure conditions STP). The maximum flow rate going through **$SVPC_d$** is thus limited by the aperture of **F_{i_LF}** and is about 700 mL/min. To overcome this limitation when a high flow rate flushing is needed, a by-pass electro-valve **EV_d** has been foreseen.

The gas mix inside the detector need to be flushed permanently at low flowrate (<50 mL/min) and at low pressure (50-100 mbar) due to outgassing components. This can be made through the mass flow controller **FC_{o_LF}**. Again a by-pass electro-valve **EV_{o_LF}** has been added for flushing at higher rates principally for beamline tests at atmospheric pressure and to enhance the vacuuming of the detector. The exhaust is then connected through **EV_{ps}** to the secondary pumping station. Having two different pumping stations for the control is not obvious but in some cases it is needed : For example when the chamber is totally vacuumed (instruction 0 bar to **DVPCc**) and the detector is flushed, having only one pumping line would connect the exhaust of the flow controller to the chamber volume and then would increase the pressure in the chamber. It is possible to use only one pump and play with the opening and closing of **EV_{ps}** and **EV_{pm}** but it is much more convenient to have two independent pumping stations. Also, for automatic sequences, it will be important to control or at least to have the information about **EV_{RP}** about because root pumps play a huge role regarding to vacuuming of the instrument. Alternatively or additionally, **Pm** could be replaced by **RP**.

Prototyping setup

Figure 2 is a picture of the prototype set up at the ILL. For the tests, dummy vessels withstanding more than 1 bar overpressure have been used. The volumes for each of them are far from what could be the real ones but it was much more easier to implement. Also the constraints in terms of pressures peaks and oscillations are much larger in that case than with bigger vessels, which means that a good operation in that conditions should guarantee a good operation at full-scale.

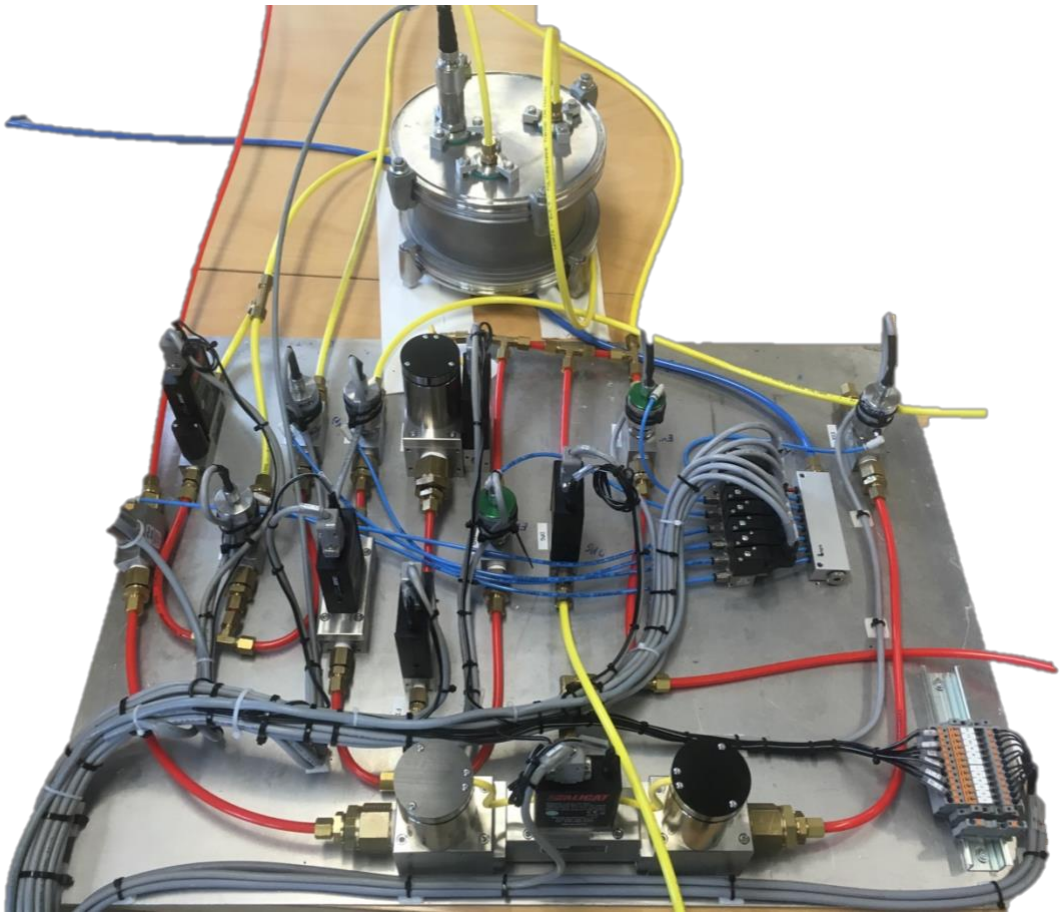

Figure 2: Picture of the gas control system components on the connector board

All the piping has been made with standard Legris® connectors and with ∅8 mm-polyamide and polyester tubes. We can already noticed here that some pipes (i.e. vacuum lines) should be adapted – with bigger diameters – for full-size tests to enhance the performances of the device.

All the components for the gas system are listed in the following table. Each controller comes from ALICAT manufacturer and is equipped with a MODBUS-RTU communication protocol to communicate with the Ladder-based programmable logic controller (PLC). A picture of the electric control panel is given in Figure 3. The PLC from PLSystems is embedded in the 10" HMI touch screen on the front of the electrical panel. We chose to use the PLSystems solution because of the license-free programming software rather easy to use. The PLC is

provided with a 8 Gb SD card to store any relevant information (alarms, documentation, logs, screenshots, etc.).

The pneumatic valves are all provided with end-switches and each is triggered by an 0-24V electro-valve connected to the compressed air grid. A special attention should be paid to **EVs** that ensures the safety of the system; it might need to be replaced by a bigger valve depending on the respective volumes at full scale of the chamber and the detectors.

Table 1: List of the components of the gas control system

Type	***Component Name***	***Characteristics***	***Communication***	***Reference***
Pneumatic-Valves	Evs	N.O. + end switches	0-24V DC	APTech AK series
	Evps	N.C. + end switches	0-24V DC	APTech AK series
	Eva	N.C. + end switches	0-24V DC	APTech AK series
	Evg	N.C. + end switches	0-24V DC	APTech AK series
	Evd	N.O. + end switches	0-24V DC	APTech AK series
	EVo_HF	N.C. + end switches	0-24V DC	APTech AK series
Mass flow controller	FCo_LF	100 SCCM/min	MODBUS-RTU	ALICAT Mass flow controller
Mass flowmeters	Fi_HF	100 SCCM/min	MODBUS-RTU	ALICAT Mass flowmeters
	Fi_LF	50 SL/min	MODBUS-RTU	ALICAT Mass flowmeters
Pressure controllers	SVPCd	external Pressure gauge 4-20 mA driven	MODBUS-RTU	ALICAT PC3-EXTSEN
	DVPCc	internal Pressure gauge	MODBUS-RTU	ALICAT PCRD3
Pressure gauges	PGd1	Absolute	4-20 mA	ALICAT P series
	DPG	Differential	MODBUS-RTU	ALICAT P series
Automation HMI				10 ’’ Unitronics + 8Gb SD

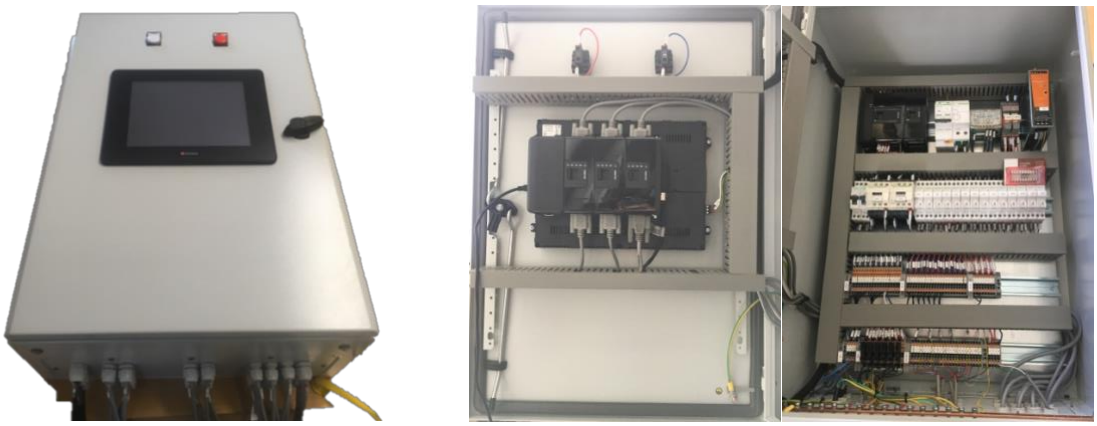

Figure 2: Pictures of the electric control panel with HMI screen.
In the middle, one can see the back of the controller with 6 RS232 ports for communication with the ALICAT controllers. Other extension boards (with analog input output and on/off- relay outputs) are mounted on a DIN rail (right picture, left top corner)

The whole setup, including the electric panel and the connector board should then be stacked onto a dedicated carriage (see model on Fig. 3) so that it can be easily moved to any experimental area.

Functional specifications and requirements

At the beginning of the study, the only requirement was to be able to operate the detector in safe conditions. That means the user should be able to activate valves, to fill, to empty or to change the pressures and flow rates inside the volumes only if it does not compromise the safety of instruments. This kind of operation stays manual but with automatic safety.

It has also been added some other features that correspond to automatic sequences the user is supposed to use frequently for tests. In practice these sequences, defined in the following sections, are routines like vacuuming the vessels and the chamber at the same time or go from vacuum to atmospheric pressure gradually and safely, etc.

In addition to that, a screen allowing the monitoring and recording of all data has been made so that the user can easily follow the system behavior in time.

Figure 3: 3D model of the carriage supporting the connector board and control panel.

Stable and transitory states of the system

In order to identify the requirements in terms of automation, a list of stable states of the system and the transitions in between has been made. These stable states are listed below:

Table 2: List of stable states

Stable States	Gas and Pressure		Comments
	Chamber	*Detector*	
S0a	Soiled air / 1 bar		Setup ready - No power supply
S0b	Soiled air / 1 bar		Setup ready - Power supply
S1	Vacuum		Setup entirely purged
S2	Soiled air / 50 mbar	Vacuum	Setup partially purged
S3a	Dry air / 1 bar	Gas mix /1 bar + 10 mbar	High flow rate flushing of the detector
S3b	Dry air / 1 bar	Gas mix /1 bar + 10 mbar	Steady state of the detector
S4a	Dry air / 50 mbar	Gas mix / 50 + 10 mbar	Steady state (S.S.) detector (no flush)
S4b	Dry air / 50 mbar	Gas mix / 50 + 10 mbar	S.S. detector (low flow rate flush)
S5a	Air or Mix gas + air / same pressure 0- 1 bar		Incident - EVs open - No P.S.
S5b	Air or Mix gas + air / same pressure 0- 1 bar		Incident - EVs open – P.S.

Every single state is characterized by a unique set of valves positions and sensors information that are given in appendix 1, so that the controller can identify the status of the system at any time except when the power supply is turned off. In the latter case, the user has the necessary means to restart the system. The transitions – listed in the table 3 – between two stable states are described by a set of successive actions that can be found in Appendix 2.

Table 3: List of transitory states

Transitory States	Gas and Pressure		Comments
	Chamber	*Detector*	
T0a0b	Air / 1 bar		The system is powered on
T5a0a	Air - Mix gas / 0-1 bar		From system failure to safe mode
T5b0b	Air - Mix gas / 0-1 bar		From system failure to safe mode
T0b1	Air / 0-1 bar		Complete purge of the system
T0b2	Air / 0,05-1 bar	Air / 0-1 bar	Partial purge of the system
T0b3a	Air / 1 bar	AIr- Gas mix / 1-1,01 bar	High flowrate flushing of the detector
T14a	Dry air / 0-50 mbar	Gas mix / 0-60 mbar	From complete purge to steady-state
T24a	Air / 50 mbar	Gas mix / 0-60 mbar	From partial purge to steady-state
T3a3b	Air / 1 bar	Air - Gas mix / 1,01 bar	From flushing to steady-state (1bar)
T4a4b	Air / 50 mbar	Gas mix / 60 mbar	Handling the flowrate
T30a	Air / 1 bar	Gas mix – Air / 1,01-1 bar	Steady state to safe mode
T40a	Air / 0,05-1 mbar	Gas mix – Air / 0,05 -1 bar	Steady state to safe mode

Risk analysis

In case of any failure or if some parameters go out of the defined range, then the controller has to put the system in safe mode. Thus, it is necessary to look after the risks and problems that may cause damages to the detector and to the environment. This risk analysis can be divided in two parts: the first one for the global risks that can happen at any time and the second one for the issues occurring during transitory states. We will only focus here on the first category since the other one will be considered independently for each sequence corresponding to a transition. One can also consider to define some incompatible states, preventing for example in manual mode from powering up the High Voltage Supply when **EV_s** is open.

The tables 4 and 5 list the different implemented safety functions in the PLC. Those actions have been hard-coded into the PLC but the user still has the possibility to change the threshold for the limits (see section "program description")

Table 4: Global risks

Risks	Description	Actions
RG1	Global electrical failure	Normally Open safety valve EV_s
RG2	Partial electrical failure (valves only)	Conflicting status: EV_s open – HT & BT on. Immediate shut down of BT & HT
RG3	Temperature or Humidity over the threshold defined for steady-state	Conflicting status Successive shut down of HT & BT
RG4	Too low pressure in the TOF Chamber Electronics is not enough cooled down	Successive shut down of HT & BT
RG5	Too high gas flowrate $Fi_{\_LF} > 50$ mL/min for S3b – S4a /S4b $Fi_{\_HF} > 25$ L/min for S3a	Closing of gas supply valve EV_g
RG6	Pressure differential DPG over the limit	Immediate shut down of BT & HT Opening of safety valves EV_s + Ev_d Closing of gas supply valve EV_g

Table 5: Incompatible states

Parameter 1	Parameter 2	Actions
HT – on	Stable states	Compatible combinations: HT-on & stable state S3b – S4a – S4b
HT - on	EVs open	Shut down HT then BT
T° > limit	BT – on	Shut down HT then BT
H > limit	BT – on	Shut down HT then BT
DPG > limit	-	Open EV_s
$Fi_{\_HF}$ > limit	FC_{o_LF} & EV_{o_HF} closed	Close EV_g

HMI - Program description

In this section I will describe the main features of my program implemented in the PLC particularly the actions that the user can do through the HMI. The HMI has 6 accessible user screens in addition to Unitronics screens:

Unitronics screens (Fig. 4): These screens constitute the menus where the user can parametrize inline the HMI. They can be accessed by holding the finger on the right top corner of the screen and select "Unitronics Apps".

Figure 4: Unitronics Apps

Main (Fig. 5): It sums up all the information about the system and links all the different screens together. On this screen, the user can start any transition from one stable state to another if "auto mode" is activated. Only the allowed stable states are "touch-enabled" and displayed in a red square. The program of the sequences can only be accessed with a computer (See next section)

The "STOP" button put the system in safe mode and can be used as an emergency stop. The "ACK" button allows to acknowledge any alarm that has been triggered due to any issue on the system. The acknowledgement is taken into account only if the cause of the alarm has been suppressed. When an alarm is triggered, a message describing what is going wrong is displayed on the top of every screen. Also, the user can access any time to the alarm log tapping on the top left corner of a screen. This log is also stored permanently on the SD card embedded on the PLC. The numbers in the white squares indicate the step number of the corresponding transition.

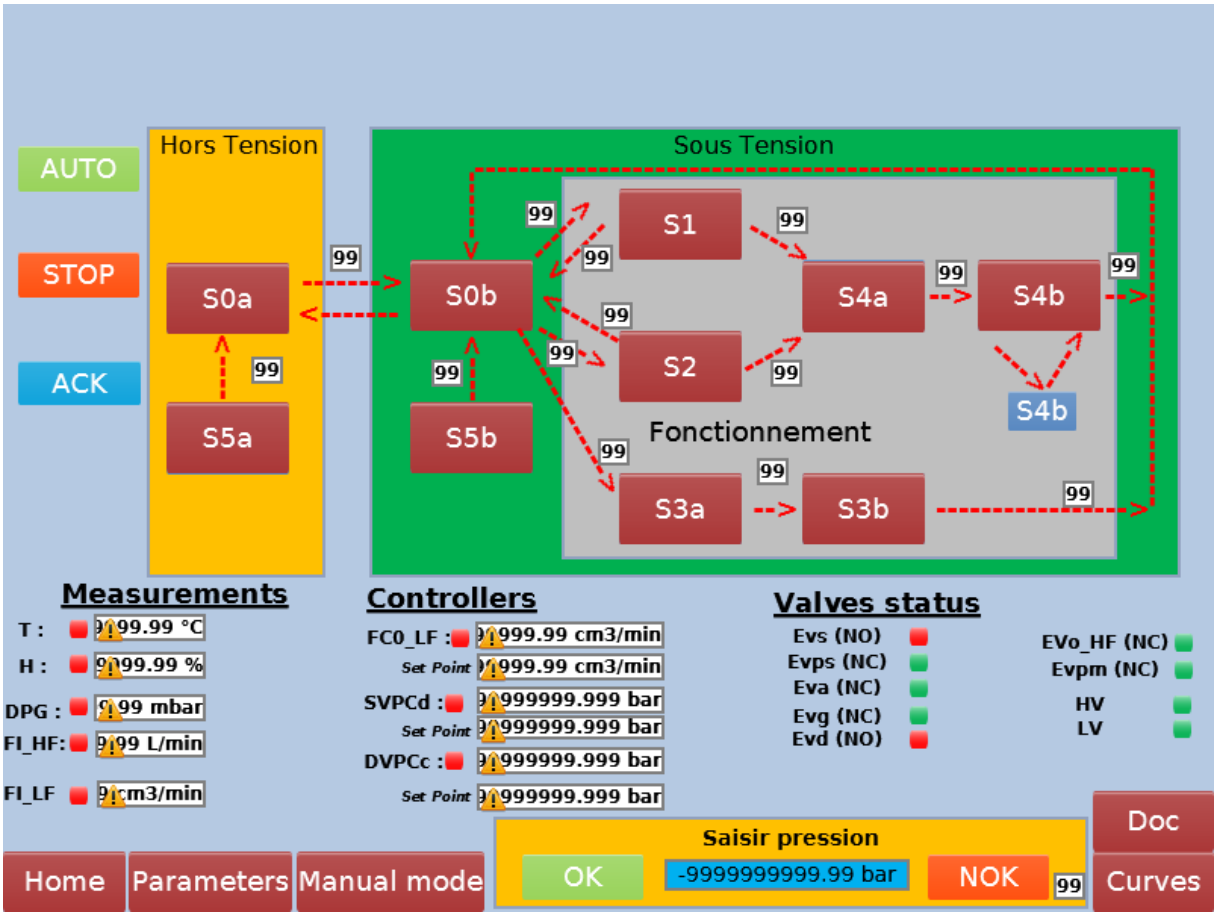

Figure 5: Home screen of HMI

Parameters (Fig. 6): The user can change here each limit fixed in the program for automatic safety. For DPG, two limits have been considered for over and under-pressure of the detector. The value measured by DPG considering the actual connections is the pressure of the chamber minus the pressure of the detector. The limits need to be set accordingly.

Figure 6: Parameters screen of HMI

Manual Mode (Fig. 7): To activate this mode, the user needs to tap on "Manu" button first. On the contrary a click on "Auto" button inactivates the manual mode. While Auto mode is chosen, valves cannot be controlled manually and new instructions cannot be sent to the controllers.
The small red square next to ALICAT controllers symbols only appear in case of communication default. The status of any valve – returned by end-switches – is visualized directly on the valve symbol: A closed valve will always have a transparent background and a red contour whereas an open valve will have a green contour and a colored background.

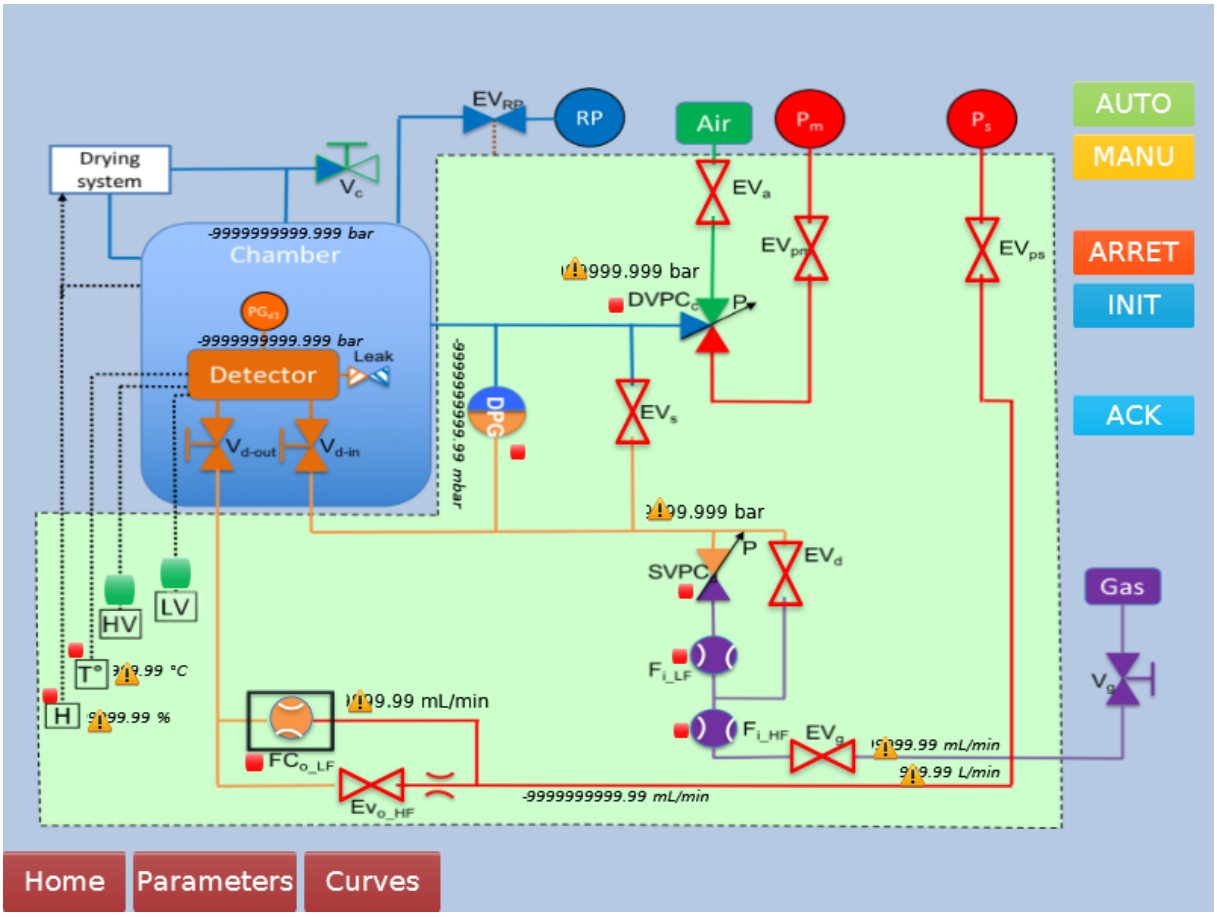

Figure 7: Manual mode screen of HMI

Regarding the values displayed on the screen, the ones next to the active controllers (**$DVPC_c$**, **$SVPC_d$** and **FC_{o_LF}**) are the set points. Those can be changed tapping on the value; then, a keyboard pops up and the user can enter a new value and click ok.
The values along the pipe lines, and the pressures in the chamber and detector "squares" correspond to measurements.
The last button is the one called "INIT". This is a specific button used at beginning for tests that allows to reinitialize a sequence launched in *auto* mode to the previous stable stable. It can be useful if a sequence is stuck at a specific step.

Curves (Fig. 8): On this screen, one can monitor in live the values of the pressures, flow rates etc. The live display can only show 4 trends at the same time. Here, the 4 curves are (**$DVPC_c$**, **$SVPC_d$**, **FC_{o_LF}** and **F_{i_LF}**). Only one axis is allowed; To see the correct units the user needs to click on "Next Curve" to select the right one and have the corresponding Y-axis. By default the ranges are the same for **$SVPC_d$** and **$DVPC_c$** (0-150 mbar). The other ranges are -100 – 100 mbar for **DPG**, 0-150 mL/min for **FC_{o_LF}** and **F_{i_LF}** and 0-1 L/min for **F_{i_HF}**.
In addition to this live mode, a recording mode is also available. To enter this mode, the user needs to click on "Live mode running" button that will immediately change in "record mode running". From there, 3 new buttons appear: "Start Sampling", "Pause Sampling" and "Clear Log". The difference with live mode is that from the moment the user click on "Start Sampling", a file will be created and opened on the SD card and the data from all controllers will be saved each 5 seconds. The display then begins to display every recorded data. The recording stops when the "Pause Sampling" button is activated and restart with another click. "Clear log" allows to delete all the data written in the current file. Attention: no data is saved until the user click

on “Stop Sampling” (same button as “Start Sampling”). Starting a new sampling will create another file and a new set of data can be taken.

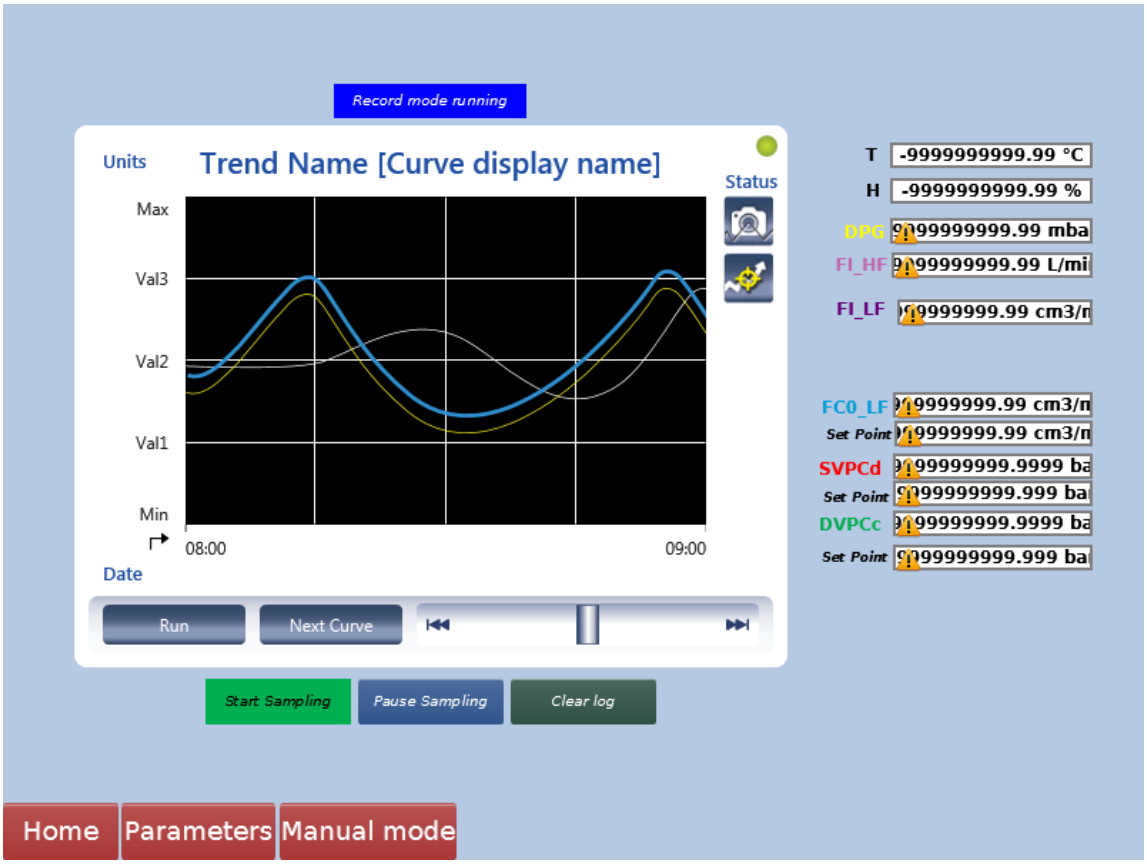

Figure 8: Curves screen of HMI

In future development, when the setup is installed on a specific experimental area with a network connection, an interesting feature easy to implement would be to automatically start and stop data sampling every X minutes to create different files and store them on a server as it goes along. On the graph, the button “Stop” do not stop the recording but only the refreshing of the display. It allows the user to select and look over the different curves and values along time.

Documentation: This screen only stores this document so that anyone can look for information. Additional documents could be added in the future.

Program structure and modifications

The program can be modified at any time but requires a computer with Unilogic software installed and plugged to the Unitronics PLC with an USB cable on the specific “Usb device” port. Then, the user need to open the project on the software corresponding to the version of the PLC. This can be done either by browsing the file on the computer or by using the “Upload” button on the software. From there, any modification can be made, any feature can be added for future developments. To apply the changes, one need to make a “Full Download” of the program to the PLC.

The structure of the program is defined by many different functions all executed at the same time. Each of this function is commented to explain the subsequent actions so there is no need to go into details here. A short notice though: there is also the possibility to create User

Defined Functions that can be re-used in the other functions (Please refer to UDFB in the help module). This has not been done here but could be interesting, i.e. to increment gradually and at the same time the pressure in the detector and in the chamber.

Each automatic sequence has its own function. The number of the executed step in this function corresponds to the one on the diagrams in Appendix 2. This is probably here that some values will need to be adjusted considering a future full-scale experiment with this apparatus. Also, there are some possibilities to implement SMS or Emails alerts or web/local/VNC server communications.

Tests of the system

To check the well-behavior of the system, some tests have been made to control that the safety routines implemented were working fine and that the system fulfills the main features required. Referring to the tables 4 and 5, each considered failure has been successfully handle by the system. The response time is about 100 µs for communication, so the shutdown and closing of the valves is immediate. The return to pressure equilibrium is a bit more difficult to evaluate. Since it strongly depends on the volume used. In this particular case with those particular diameter of pipes, the equilibrium between the detector (4 L) and the chamber (25 L) is obtained in few seconds when the differential pressure is above 50 mbar and **EV_s** opens.

This is illustrated by the Figure 9 that shows in red the pressure of the detector and in green the one of the chamber. At the beginning, the pressure in the chamber was maintained at 40 mbar and detector at 60 mbar. Then the chamber has been pumped out so that the differential pressure increase. At the moment this goes above 50 mbar, **EV_s** opens and the two volumes are pumped out at the same time. Then, when defaults were acknowledge, new values are sent to the controller and one can see that the steady state is obtained quite fast, either for the pressure or for the flow rates.

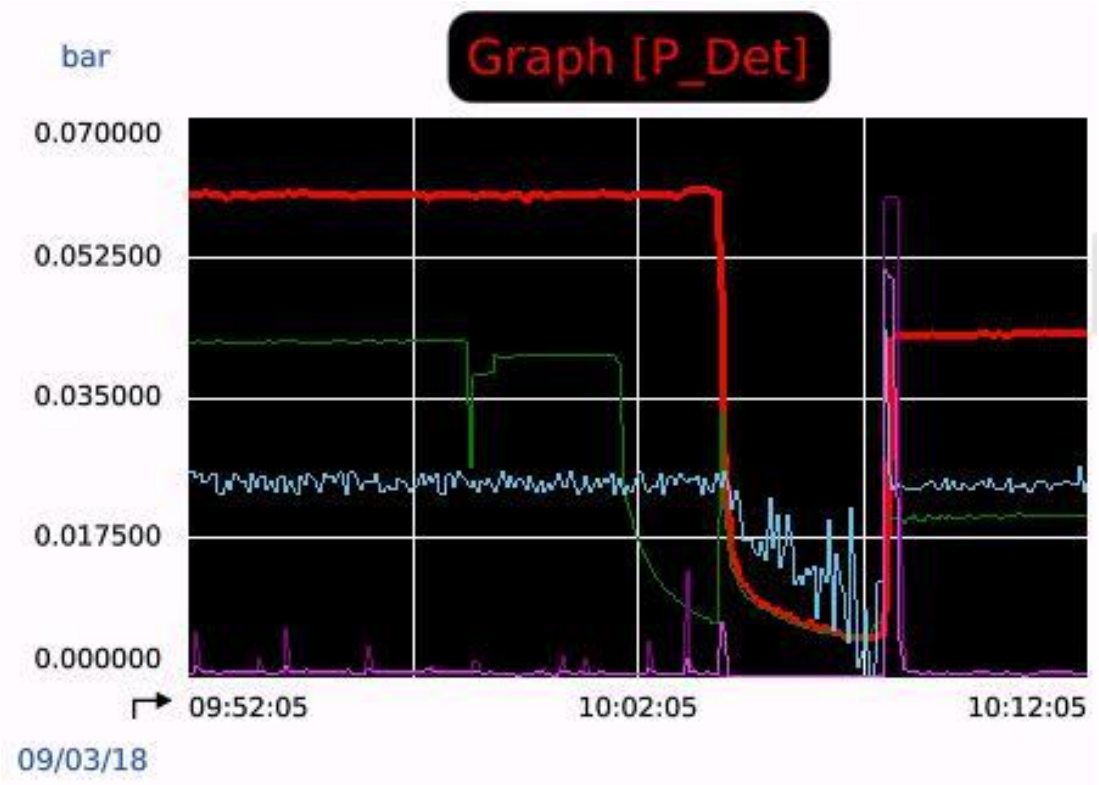

Figure 9: Screenshot of the graph displayed by the HMI. (The colors of the curves correspond to the ones on the caption on the plot Fig. 8)

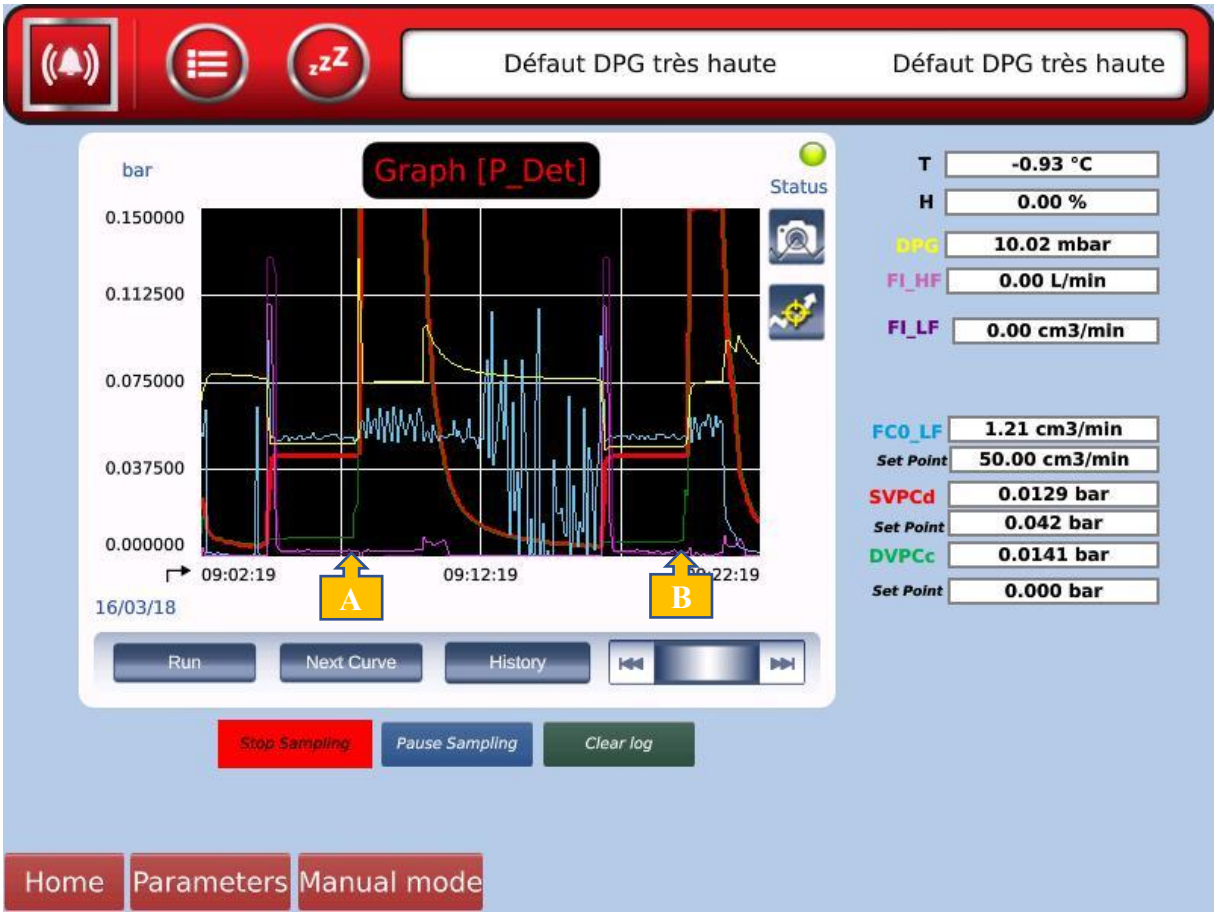

Figure 10: Screenshot of the HMI when simulating accidents.

More sudden and violent accidents have also been tested (Fig. 10). The chamber and detector are both pumped out and then the detector is filled at 42 mbar of gas. At point "A", a big leak on the chamber is made. The pressure in the chamber increase very fast and the differential pressure rapidly overcomes the limit fixed here at +150 mbar. At this moment EV_s opens and we can see on the graph that the differential returns quickly to 0 mbar. The same procedure is repeated next (Leak created at point "B"), but this time the limit for differential pressure has been fixed at 50 mbar. This time the response of the system is even faster since we cannot notice the overshoot of DPG (due to sampling time interval), and the equilibrium of pressures is obtained immediately. Those tests confirm that the system is reactive enough to guarantee safety in case of sudden and violent accident.

Another important point regarding the control of pressures regards the PID optimization. The system is made to work with bigger volumes with higher inertia, so it was a bit difficult to find PID values that allow a good performance of the pressure control. Definitely, the values of these parameters must be changed once the volumes will be different so we will not go too far in the details of these values. To change them, the user needs to access to ALICAT controllers' menu, and find "PID". For $SVPC_d$, a simple "PD" algorithm is used and this should stay that way. For $DVPC_c$, a more complex algorithm is used and P, I and D parameters can be tuned. In this test setup, the chosen and best values result in a small overshoot of 2 mbar when the detector pressure is increased from 0 to 40 mbar. Then the "overpressure" is released through FC_{o_LF}. It takes several minutes to return at the pressure instruction depending on the defined flow rate at the outlet. Then, the system perfectly maintain the pressure in the detector according to the pressure instruction of the controller.

This is illustrated by the figure 11; The red curve is the detector pressure. The flow rate at the outlet is also quite constant – around 50 mL/min – and one can see in purple the gas injection at the inlet. The test has been running all a night long and the pressure remain constant.

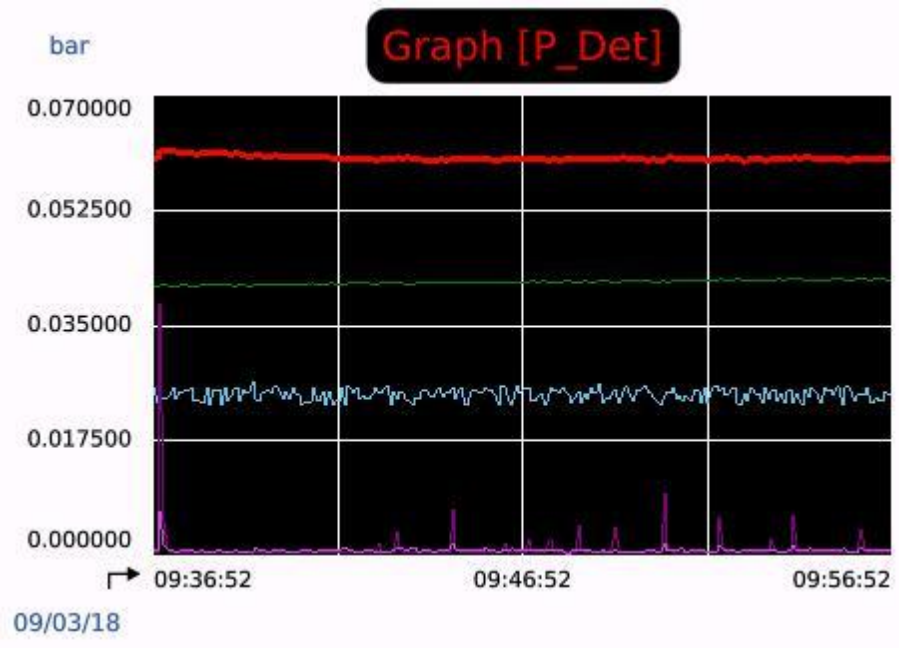

Figure 11: Screenshot of the HMI plots when system is in steady state

Another important point about pressure overshoot is the dependence regarding the starting and ending parameter values. Indeed, if the user increase the pressure instruction from 40 to 42 mbar, it results in a higher overshoot (about 6 mbar) than from 0 to 40. This is not really understandable since the pressure control operates smoothly when the instruction is not changed (Fig. 10). But once again, the effect should be greatly reduced when using much bigger vessels.

Conclusion and prospects

The aim of this study was to demonstrate the feasibility of an automated gas control system that would allow to guarantee the safety of operation of a detector composed of a poor-resistance-to-pressure vessel in a vacuum chamber. Different *scenarii* of accidents have been tested and all demonstrate the coherent behavior of the automaton. Also, the stability of pressure control has been evaluated and tests show satisfying results

Nevertheless, we saw in this document that all of this was made with a test setup that is definitely not at scale compared to the size of an actual detector or chamber. The small deviations noticed during the tests should disappear from the moment the experiment is composed of bigger vessels (because the system is designed for this) and there is no doubt about the fact that this can only enhance the performance of the device. However, this might require to adjust some PID parameters in the controllers and also to change some pipes to increase their diameter. This means that more qualification tests are needed with this prototype to prove its ability to fulfill the desired feature.

Since it was made for operating Multi-Grid detectors, the best option would be to use this system with a Multi-Grid vessel installed in an instrument. Such a test could justify to consider to build vessels withstanding only few hundreds of millibars – instead of 1 bar currently – and thus greatly reduce the weight and the complexity of the Multi-Grid detector vessels.

Appendix 1 : Stable states

Stable States	Valves												
	Ev_s	$DVPC_c$ supply	$SVPC_d$	Ev_d	Ev_g	Ev_a	Ev_{ps}	Ev_{pm}	FC_{o_LF}	EV_{o_HF}	V_c	$Vd_{\_o}$	$Vd_{\_i}$
S0a													
S0b		0.95-1.05 atm	1 atm										
S1		0-0.02 atm	60 mbar +/- 3%										
S2		50 mbar +/- 3%	0-1 atm										
S3a		0.98-1 bar	1.01-1.02bar										
S3b		0.98-1 bar	1.01-1.02bar						50 mL/min				
S4a		50 mbar +/-3%	60 mbar +/- 3%										
S4b		50 mbar +/-3%	60 mbar +/- 3%						<50 mL/min				
S5a ~ S0a		*0-1 atm*											
S5b		*0-1 atm*	0-1 atm										

Green: open, Blue: does not matter, Red: closed, Orange: variable

Stable States	Electrical signals - Sensors										
	F_{i_LF}	F_{i_HF}	FC_{o_LF}	PG_{d1}	PG_c	DPG	T°	H	LV	HV	Power S.
S0a	*0*	*0*	*0*	1 atm	1 atm	0	25°C	40%	off	off	no
S0b	*0*	*0*	*0*	1 atm	1 atm	0	25°C	40%	off	off	yes
S1	*0*	*0*	*0*	0 atm	0 atm	0	25°C	0%	off	off	yes
S2	*0*	*0*	*0*	0 atm	50 mbar	50	25°C	~0%	off	off	yes
S3a	*~0*	*25 L/min*	*~0*	1 bar	1 bar	0	25°C	~0%	off	off	yes
S3b	*50 mL/min*	*~0*	*<50 mL/min*	1,01 bar	1 bar	10	35°C	> 0%	on	on	yes
S4a	*< 50 mL/min*	*~0*	*0*	60 mbar	50 mbar	10	35°C	> 0%	on	on	yes
S4b	*< 50 mL/min*	*~0*	*<50 mL/min*	60 mbar	50 mbar	10	35°C	> 0%	on	on	yes
S5a	*0*	*0*	*0*	0-1 atm	0-1 atm	0-30	25°C	> 0%	off	off	no
S5b	*0*	*0*	*0*	0-1 atm	0-1 atm	0-30	25°C	> 0%	off	off	yes

Appendix 2 : Automatic sequences

The numbers correspond to the step numbers of the corresponding transition in the program loaded in the PLC. When numbers are missing this is due to some modifications or empty spaces to add more features in the future.

S5b->S0b, S1->S0b, S2->S0b: Atmosphere pressurizing

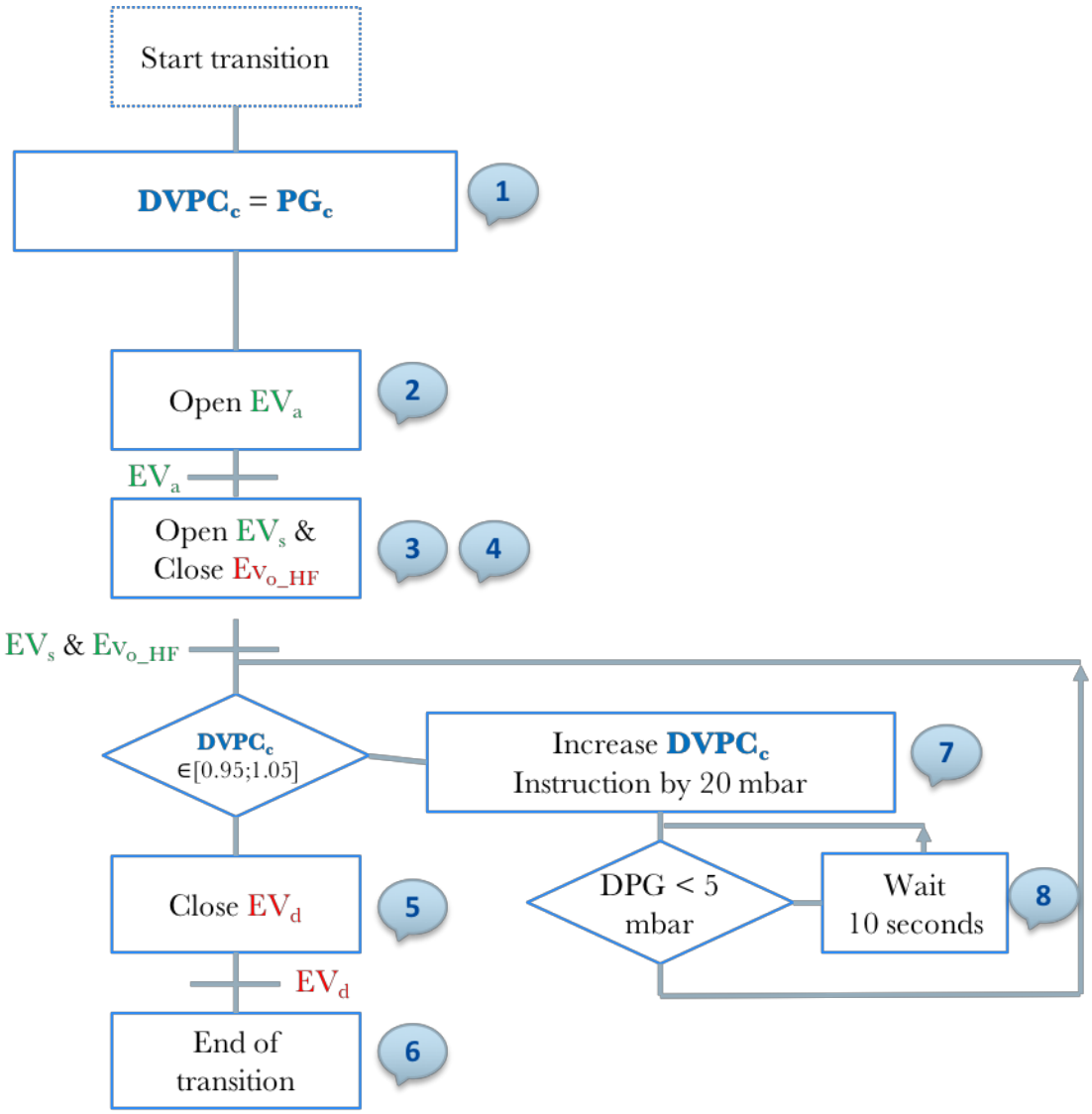

S0b->S1: Total vacuuming

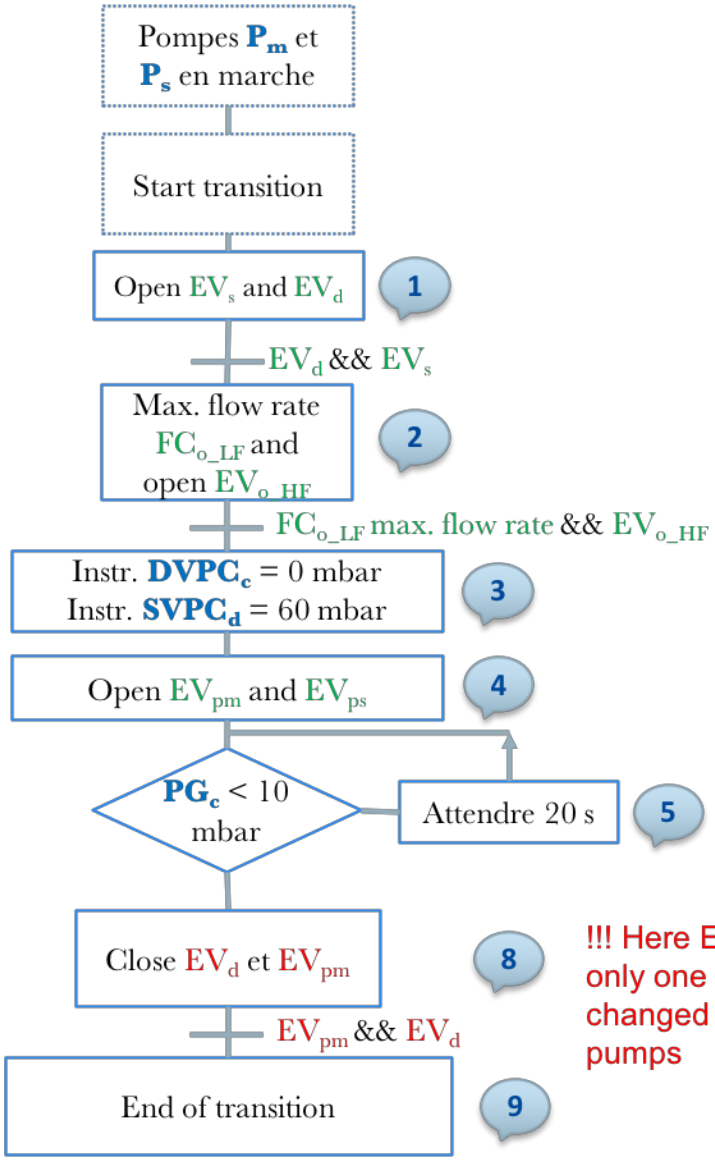

!!! Here Evpm is closed because only one pump is used. Should be changed afterwards with two pumps

S0b->S2: Partial vacuuming

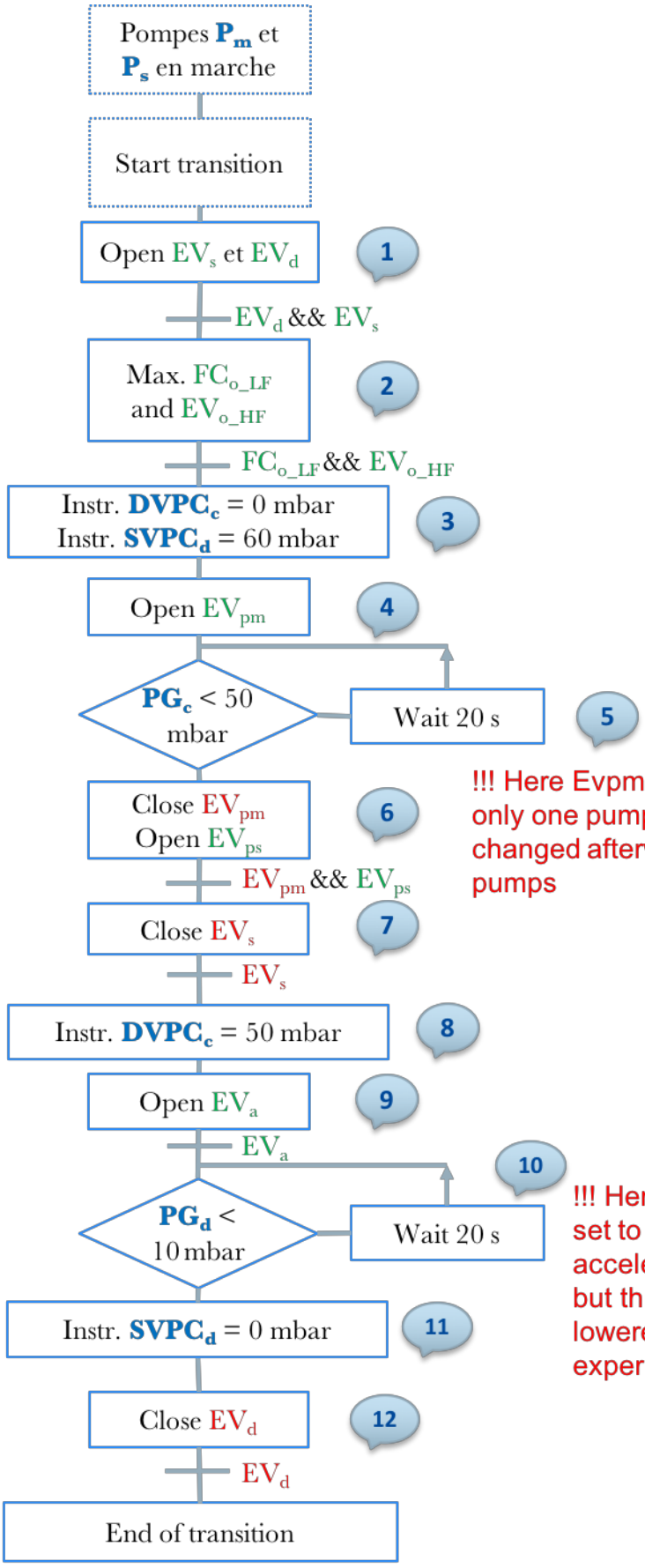

!!! Here Evpm is closed because only one pump is used. Should be changed afterwards with two pumps

!!! Here the limit has been set to 10 mbar to accelerate the operation but this value should be lowered for a real experiment

S0b->S3a: High flow rate flushing

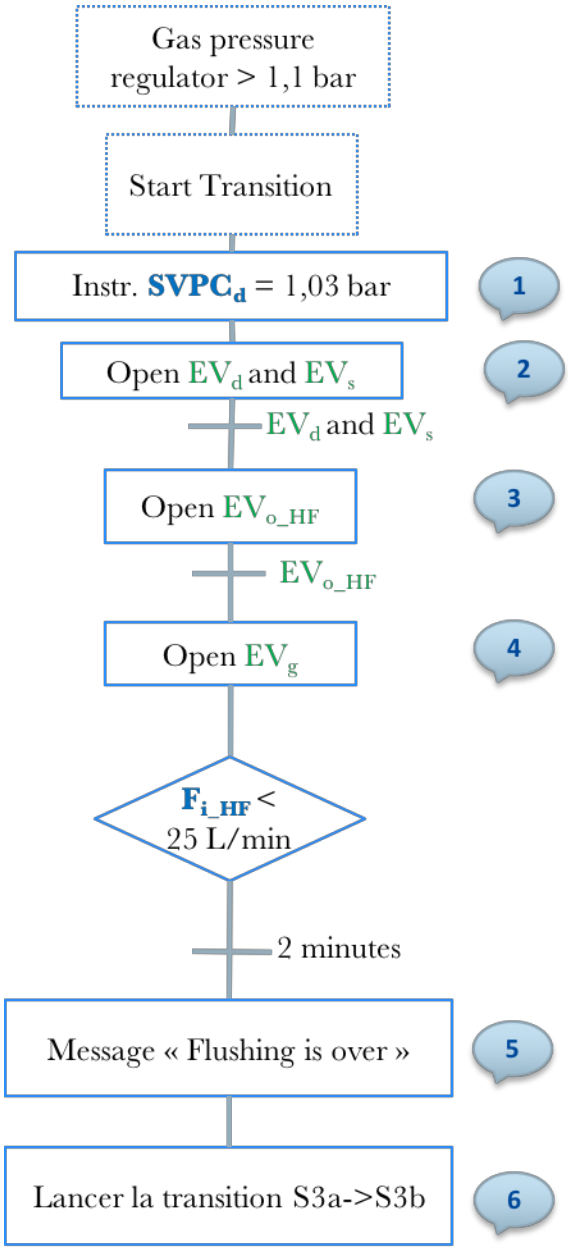

S3a->S3b: Atmospheric pressure steady state

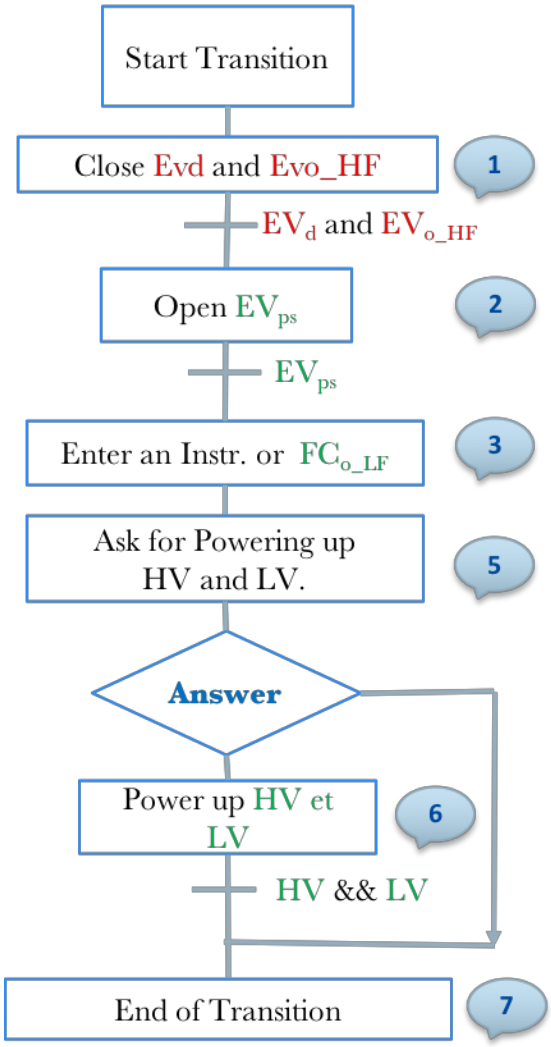

S1->S4a: Detector-Chamber Filling

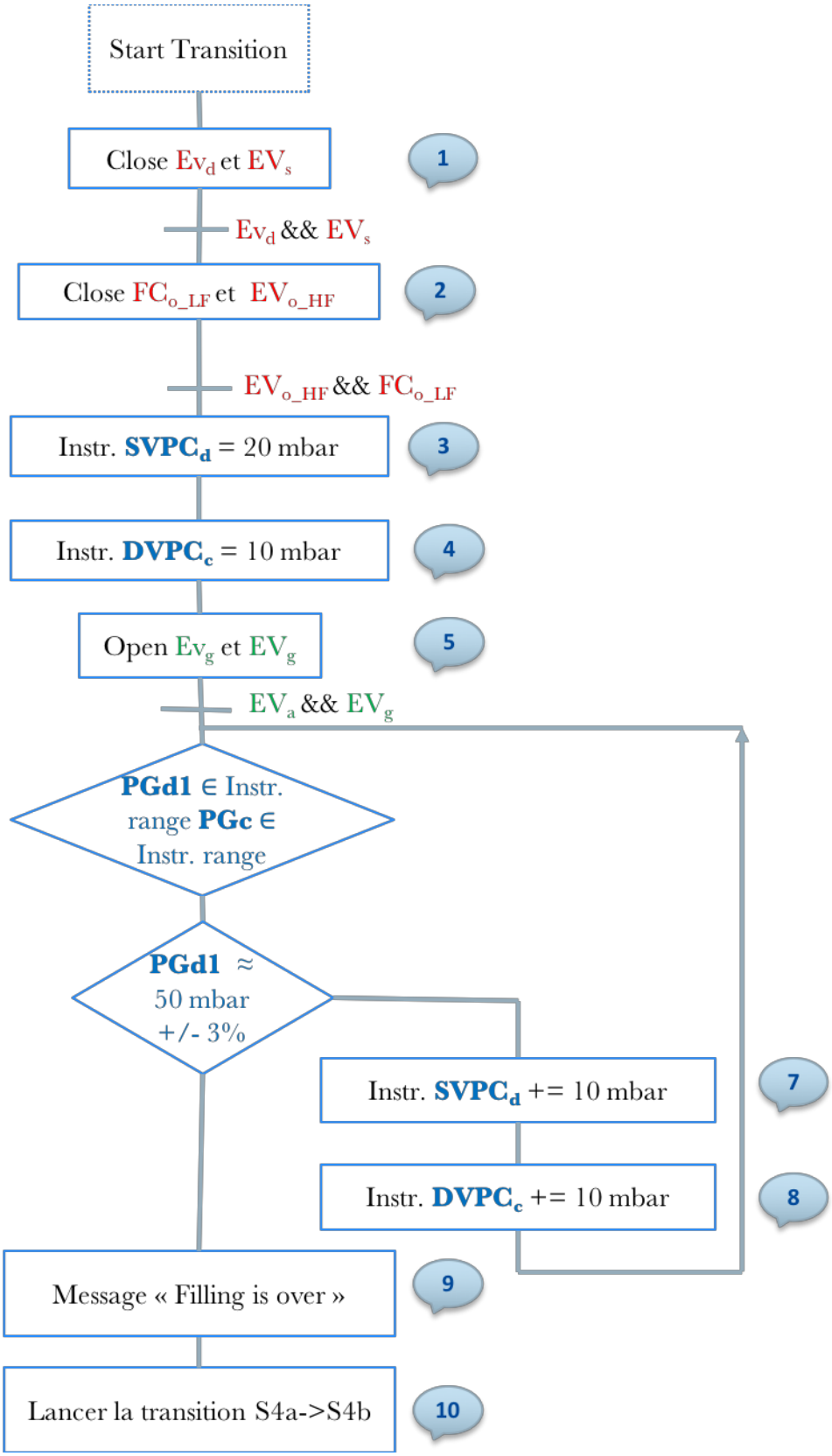

S4a->S4b: Start Low flow rate flushing

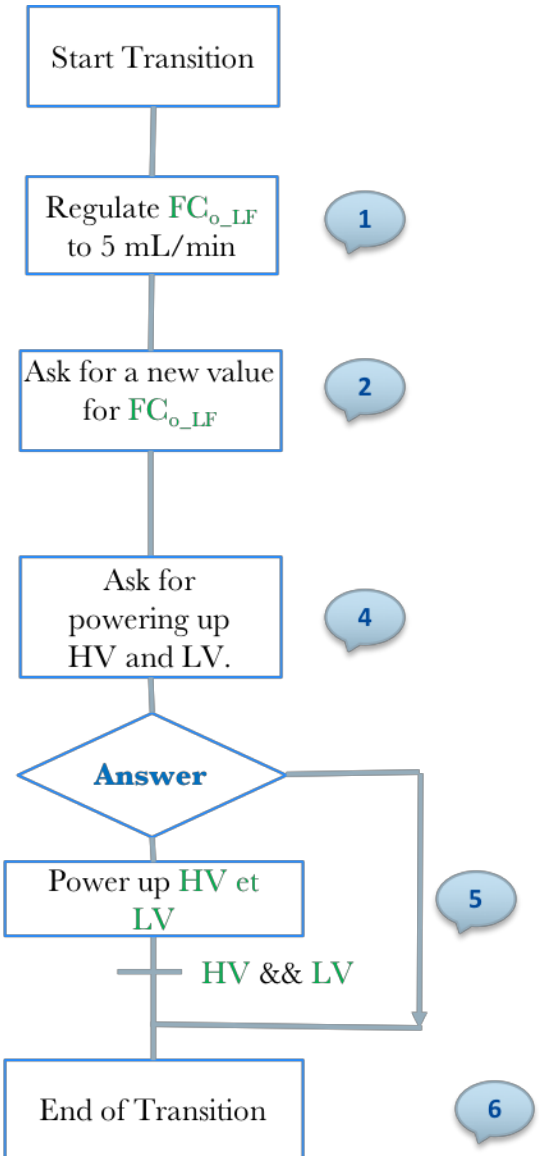

S2->S4a: Detector Filling

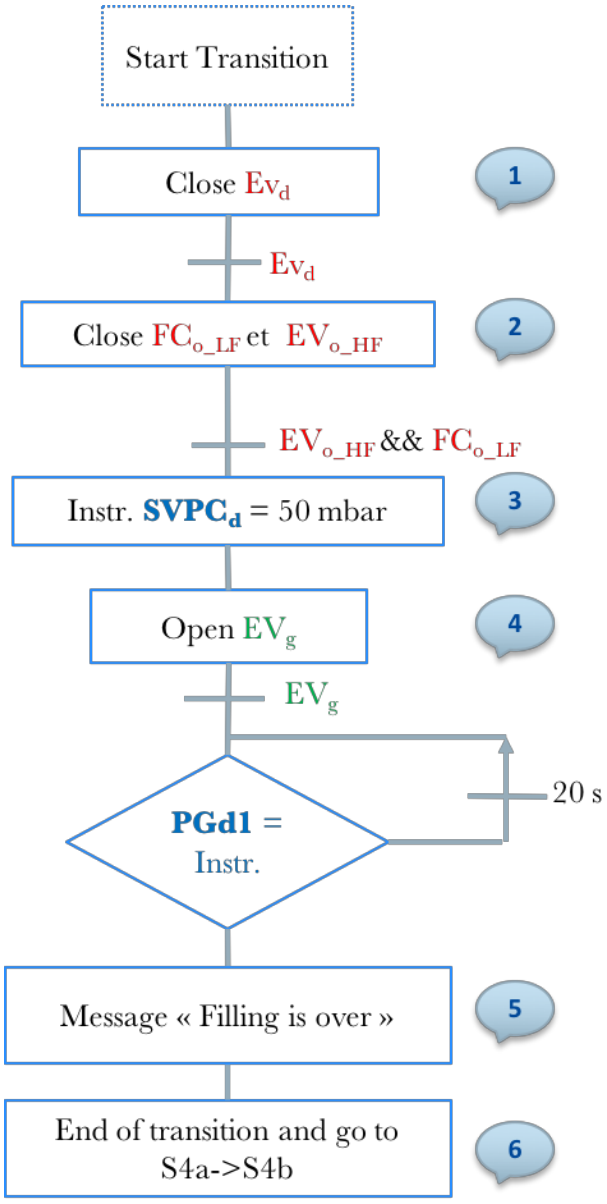

S3b->S0b or S4b->S0b: Return at atmospheric pressure.

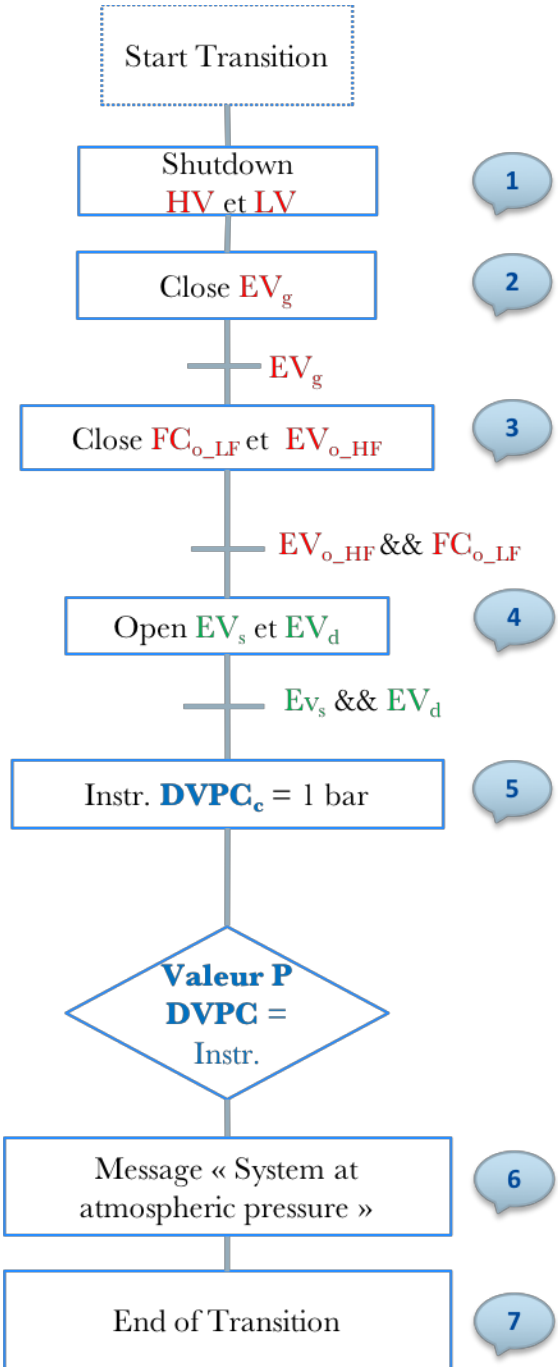

S4b->S4b: Change detector pressure.